1-1-2009

Laser induced reverse transfer for microfabrication

Gurinderpal Singh Dhami
Ryerson University

LASER INDUCED REVERSE TRANSFER FOR MICROFABRICATION

By

Gurinderpal Singh Dhami

Bachelor of Engineering, 2002

Punjab Technical University, India

A Thesis

Presented to Ryerson University

In partial fulfillment of the

Requirements for the degree of

Master of Applied Science

in the Program of

Mechanical Engineering

Toronto, Ontario, Canada,2009

AUTHOR'S DECLARATION

I hereby declare that I am the sole author of this thesis report.

I authorize Ryerson University to lend this thesis to other institutions or individuals for the purpose of scholarly research.

Gurinderpal Singh Dhami
Department of Mechanical and Industrial Engineering
Ryerson University

I further authorize Ryerson University to reproduce this project by photocopying or by other means, in total or in part, at the request of other institutions or individuals for the purpose of scholarly research.

Gurinderpal Singh Dhami
Department of Mechanical and Industrial Engineering
Ryerson University

LASER INDUCED REVERSE TRANSFER FOR MICROFABRICATION

Gurinderpal Singh Dhami, Master of Applied Science, 2009
Mechanical Engineering, Ryerson University

ABSTRACT

The general objective of this thesis is to introduce ultrafast "Laser Induced Reverse Transfer" (LIRT) as a technique for material transfer in micro-fabrication. LIRT is performed using femtosecond laser radiation of wavelength 515 nm with gold coated silicon wafers under ambient conditions. The material transfer process is explained by the dynamics of a laser ablated plasma plume. The influence of processing parameters such as laser pulse energy, pulse width and scan speed on the width of transferred material is also investigated. The width of the deposition increases with the increase in pulse energy while it decreases with scan speed. Also, the width increases with laser pulse width ranging from femtosecond to picosecond range. In general the transferred material size is determined by the amount of material present in the plasma plume which depends on the energy deposited in the bulk material by laser irradiation. In the femtosecond pulse width range, the increase in pulse energy at constant pulse width transfers more energy in a short time with minimal heating effect to the surrounding material. Hence, the efficiency of material removal increases. This in turn enhances the feature size. On the other hand, as the laser pulse width increases from femtoseconds to picoseconds, the interaction time of laser radiation with material increases. This leads to an increase in the amount of material removed, thereby increasing the transferred material size. However, thermal damage to the surrounding material increases. An increase in scan speed at constant pulse energy decreases the laser interaction time, which results in a decrease in amount of material in the plasma plume.

This in turn decreases the width of the deposited material. In general, femtosecond laser induced reverse material transfer is an efficient technique for microfabrication and can be used for device manufacturing.

ACKNOWLEDGMENTS

I would like to thank my research supervisors, Dr. K. Venkatakrishnan and Dr. Bo Tan, for their support, expertise, guidance and encouragement all through the course of my study at Ryerson University. They have been

a great source of inspiration during my hardships and very special thanks to them for leading me in the right path.

I would like to thank Dr. Greg Kawall, Director of Mechanical Engineering Graduate program, all the faculty members, technical officers and administrative staff members for their kind support and cooperation all the time during my stay at Ryerson University.

I am also grateful to my parents, Mr. Manjit Singh Dhami and Mrs. Manjit Kaur Dhami, brother Mr. Tejinder paul Singh Dhami and fiancée Ms. Manjit Sond for their continued moral support, prayers, love and help through the troubled times. Finally, I am grateful to the Grace of God for the countless blessings I have received.

CONTENTS

LIST OF FIGURES

NOMENCLATURE

ns	nanosecond (10^{-9} s)
ps	picosecond (10^{-12} s)
fs	femtosecond (10^{-15} s)
μm	micrometer (10^{-6} m)
nm	nanometer (10^{-9} m)
MHz	megahertz (10^{6} Hz)
W	watt
GW	gigawatt
μJ	micro-Joule (10^{-6} J)
nJ	nano-Joule (10^{-9} J)
T_i	ion subsystem temperature
T_e	electron subsystem temperature
D	Feature size
ω_0	Beam Radius
$Ø_0$	Maximum Laser fluence
$Ø_{th}$	Threshold fluence
E_{pulse}	Pulse Energy

CHAPTER 1- INTRODUCTION

1.1 Introduction to Micro-fabrication through deposition

The ability to produce a wide variety of material structures, spots and lines with high resolution at micro and submicro scales is desirable in many fields from the fabrication of biodevices, microelectronics and integrated optics to biological microarrays. The requirement of microfabrication of patterns vary with different applications but generally, it requires high resolution, simplicity, low cost, control of deposition size and thickness, high spatial accuracy and quick processing time. Many techniques have been developed to address these challenges, each with their own pros and cons. Microfabrication is actually a collection of techniques which are utilized in making microdevices. Some of them have very old origins but are not related to manufacturing techniques such as lithography and etching. To fabricate a microdevice, many processes must be performed one after the other and sometimes repeated several times. These processes typically include depositing a thin film, patterning the film with desired micro features and removing portions of the film by etching. For example, in memory chip fabrication there are almost one hundred processes involved such as lithography, oxidation, etching, doping and many more. Further, these microdevices are constructed using one or more types of thin films. Thin film deposition is a very important step in microdevice manufacturing. The kind of thin films used depend on the type of microdevice. For example, an optical microdevice has films which are reflective or transparent in nature. In the case of electronic microdevices, the films can be conducting, insulating or semiconducting.

Thin film deposition is the act of applying a thin film of material to a substrate surface. It is used for the manufacturing of semiconductors, layers of insulators, conductors to form integrated circuits, optics and packaging. There are several methods available for the deposition of thin films. They broadly falls into two categories depending on whether the primary process is chemical or physical. In chemical deposition, a compound undergoes a chemical change at solid surface and leaves a thin layer. Chemical deposition of thin films are conformal in nature rather than directional. Several types of chemical deposition techniques are available depending on the type of precursors used such as liquid, gas or plasma. Laser chemical vapor deposition is one of the known methods used for patterned deposition with high resolution. However, the requirement of high temperature and lack of suitable chemical precusors limits the deposition of different materials using this technique. Also the technique proves to be too complex and very expensive. Physical deposition uses mechanical or thermodynamic means to produce thin films. The target material to be deposited is placed in an energetic and entropic environment so that particles escapes from its surface. A cooler substrate surface placed nearby to the target draws energy from the escaped particles as they arrive closer and allowing them to form a thin layer of target material. The whole system is placed in a vacuum chamber to allow the particles to move as freely as possible. Films depositing by physical means are mainly directional rather than conformal because the particles tend to follow a straight path. Pulsed laser deposition (PLD) is the another most commonly used method for pattern deposition. In PLD, focused pulsed laser radiation vaporize the target material and convert it to plasma and is collected on the substrate surface. Another method used for deposition is photolithographic process. This process allows the fabrication of complicated structures from a wide range of materials with high resolution. The use of lithographic techniques for micro fabrication of electronic and mechanical structures

at the sub-millimeter level requires expensive equipments, extreme processing conditions, multi-step process and timescales of the order of weeks to go from design to completed device. Deposition of delicate materials (protein, DNA and other polymeric materials) require methods that can be used in ambient temperatures. Common methods for these purpose are ink-jet printing and pin spotting. However, these methods suffer from low resolution. One family of processes that are of great interest for material transfer in microfabrication are direct-write techniques. This technique allows both material transfer and patterning to be performed simultaneously. A significant majority of direct-write techniques are laser based.

1.2 Laser induced material transfer

Pulsed laser evaporation/transfer of thin film of material is successfully used for the past two decades. In this process a transparent target is irradiated by laser from the back to deposit on the substrate that is kept close to target. Laser induced material transfer is referred by different titles, such as laser direct-write (LDW), laser induced forward transfer (LIFT) (a detailed study in section 1.2.1), MAPLE-DW (Maple Assisted Pulse Laser Evaporation- Direct Write) and MELD (Microstructuring by Explosive Laser Deposition). The mechanism of the material transfer from target to substrate is very complex. The material transfer depends on type of laser, wavelength, pulse energy, pulse width, spot size, type of material and the atmosphere.

Laser direct-write is a general term that encompasses modification, subtraction, and addition processes capable of creating patterns of materials directly on substrates without the need for lithography or masks. Laser direct-write employs a laser pulse to transfer material to substrate with high resolution without the use of lithography. The best resolution achieved by direct-write techniques is ≈100 nm [1], which is better than that obtained by lithography. These techniques

are advantageous because they allow a large number of materials to be deposited and have the ability to deposite delicate materials, have quick processing times, and provide great simplicity in their usage. LDW covers a broad range of laser based processes, which are the removal (i.e. laser micromachining), addition (laser induced transfer) and annealing of wide variety of materials. This technique is used for the mesoscale patterning of materials directly on a substrate without the requirement of multi-step lithography for the fabrication of microelectronic devices. These patterned structures are used to create conductive lines in functional circuits for connection purposes. Also, the patterns obtained from direct writing can be assembled together for the manufacturing of multilayer stacked micro batteries [2]. The main reason for accepting direct writing techniques in industry is its ability to transfer materials without changing their electrochemical or structural properties under ambient conditions. Figure 1.1 illustrates laser direct-write addition technique. In this technique, material of interest in powder form combines with a liquid carrier to form an ink. This ink is spread on a glass substrate and laser irradiates the ink from behind the glass substrate to propel a mass of ink material forward onto the substrate kept below. This kind of printing process takes place either by scanning laser or moving the ink spreads glass substrate LDW techniques typically combine good resolution with simplicity and rapid processing time.

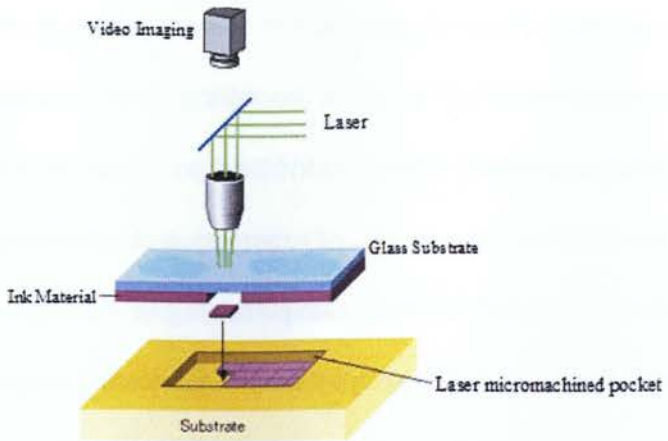

Figure1.1: Laser direct write

1.2.1 Laser induced forward transfer (LIFT)

A very promising material transfer technique offering sub-micron lateral resolution deposition of a wide variety of materials is Laser Induced Forward Transfer (LIFT). It is a subset of laser direct-write technique that uses laser to transfer material from a thin film precursor to a substrate. Laser induced forward transfer was first proposed by J. Bohandy et. al.[3] in the year 1986. They deposited the Cu lines of 60 μm at 139 mJ pulse energy and 40 μm lines at 110 mJ of pulse energy using high energy excimer laser (193 nm) on Si substrate. It was observed that the thermal ablation of the source film was the reason for material transfer onto the substrate. They also observed that the optimal fluence (pulse energy(J)/focal spot area(cm^2)) for uniform deposition was just above the ablation/transfer threshold energy, which was the minimum energy required to initiate the laser ablation. LIFT is used to deposit a variety of materials such as metals, semiconductors, dielectrics and biomaterials even at ambient conditions. It provides the benefit to transfer various kinds of thin films (aluminum (Al) [4], chromium (Cr) [5] and gold

(Au) [6], etc.) on an acceptor substrate. Schematic in Figure 1.2 shows the transfer of a thin film to the acceptor substrate. In Figure 1.3, a step by step process laser induced forward transfer is presented.

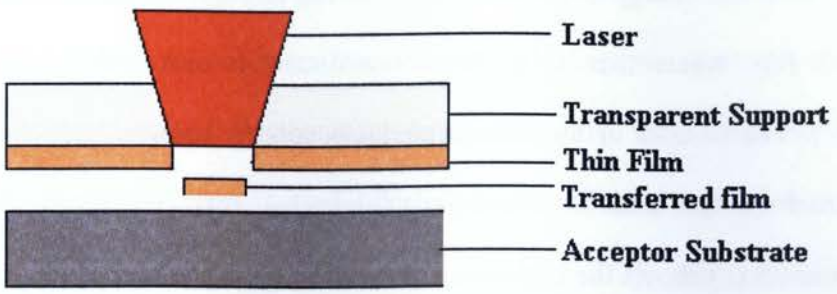

Figure1.2: Schematic of laser induced forward transfer

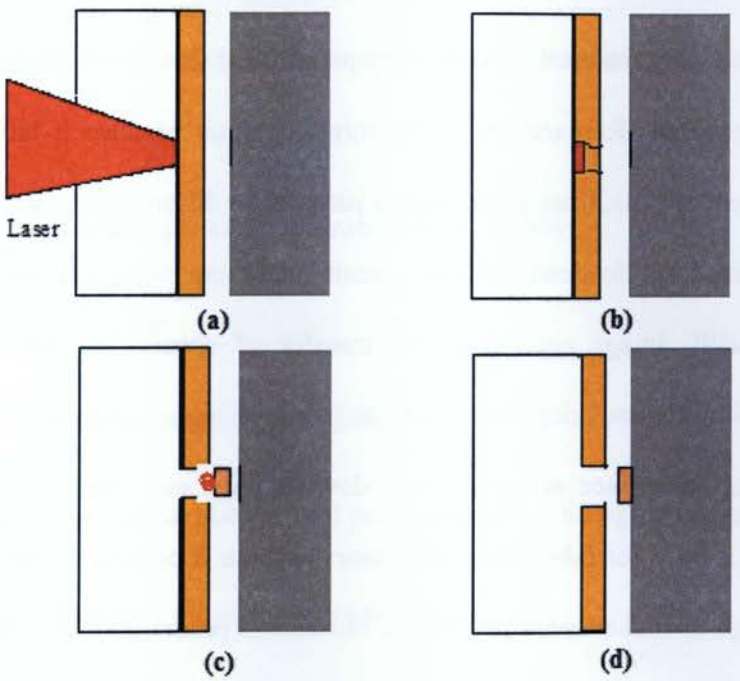

Figure1.3: Steps in laser induced forward transfer

In LIFT, the thin film to be transferred is coated onto a transparent donor substrate. The coating on donor substrate is performed using PLD (Pulsed Laser Deposition) and/or EBD (Electron Beam Deposition). The donor substrate is placed in close proximity to the acceptor substrate. A laser pulse of sufficient energy is focused onto thin film through the transparent donor substrate (see Figure1.3 (a)), where the energy from laser pulse is absorbed by thin film material (Figure1.3 (b)). The transfer of thin film material occurs by ablation process which provides sufficient thrust to the thin film material (Figure1.3 (c)) to deposit on the acceptor substrate.Figure 1.3.(d) shows the deposition of material on to the acceptor substrate. Due to its simplicity and ability to deposit large number of materials, LIFT becomes so popular for last two decades.

The ability to deposit any material that could be prepared in the form of thin film made LIFT a popular field of research. Researchers prefer this technique because it has the capability to deposit submicron-sized dots, lines and complex patterns on different substrates. It has been used in various specialized applications such as circuit interconnections [7], surface pattering [8], photo mask repair[9], image recordings by transfer of specialized inks [10], chip repair technology [11], simultaneous deposition and pattering of high-T_c superconducting films [12], frequency trimming in surface acoustic wave devices [13], and other physical technological aspects [14-19]. It is used for fabricating biosensors because it permits to deposit patterns of bio molecules with high spatial resolution [20]. In biosensors production, biological materials in a solution are used to prepare a liquid film on the donor substrate and then micro-droplets of the liquid film are transferred to the acceptor substrate by laser radiation. The solvent used in this process acts as a transport vector and prevents the decomposition of the bio-molecules [20].

Laser induced forward transfer is also used for micro printing and bioelectronics. Micro printing is an anti-counterfeiting process which is widely used in currency, bank cheques, and other money related applications. It involves printing text onto currency or other items at a size that is not visible to the naked eye. This technique can also be applied for metal films and materials that are heat resistant, sensitive materials such as biomaterials, organic dyes and semiconducting polymers that can be damaged by the laser irradiation [21]. It is used for several other applications such as rapid prototyping of microelectronic circuits, repair of microelectronic mechanical systems (MEMS) [22], fabricating capacitors [23], micro fluidics, to create conductive lines and pads for rapid prototyping and repairing microdevices [24]. Laser induced forward transfer technique is implemented to transfer more complicated materials including chemo selective polymers, organo-metallic compounds, various classes of battery materials and phosphorus.

The advantages of LIFT technique can be summarized as follows.

1.2.2 Advantages of LIFT

The following list outlines the advantages of LIFT.

- No dependence on optical and thermal properties of the acceptor substrate.
- Minimal perturbation of the acceptor substrate.
- Elimination of handling and contamination problems.
- Allows deposition under ambient conditions.

- Allows deposition of a wide range of materials including metals, dielectrics, ferrites, polymers, composites and chemically reactive materials.
- Ability to print complex patterns conformal to the surface of the receiving substrate.
- Allows transfer of complex fluids with a wide range of viscosities ranging from aqueous solutions and nano-inks to thick ceramic pastes or suspensions.
- Capable of write speeds approaching 1 m/sec with <10 μm resolution.
- Allows deposition of different materials for multilayer structures simply by exchanging ribbons.
- Ideally suited for transferring droplets of a solution containing bio-molecules without altering their biological activity. The high spatial resolution of LIFT makes it competitive in front of more conventional techniques like pin deposition and ink-jet printing [25].
- Laser induced forward transfer has great potential as it can be used for texturing of sensitive parts and pattern deposition [26].The technique generally used for pattern deposition is Laser chemical vapor deposition (LCVD). The potential of LIFT over LCVD can be realized from their comparison.

1.2.3 Laser induced forward transfer versus laser chemical vapor deposition

The use of laser induced forward transfer has a much greater advantage than laser chemical vapor deposition. These advantages of LIFT are outlined below:

a) No chemical processes are involved, allowing microelectronic quality materials to be prepared easily.

b) Transferred films can be expected to reproduce the high purity of a pre-coated (sputtered or evaporated) film.

c) LIFT can be performed under ambient atmospheric conditions.

d) No complicated vacuum deposition apparatus or gas handling systems are needed.

The disadvantages of using LCVD are the need of vacuum or gas handling systems and the use of harmful and toxic gases. The writing speed for LCVD is only a few microns per second [27], makes it limited to few applications. This problem can be eliminated by using laser-induced chemical liquid deposition (LCLD). By using LCLD writing speed can be increased and the solutions used are easier to handle than the toxic gases. But it is very difficult to remove liquid completely and cleanly from the processed surface without damaging and contaminating adjacent parts.

1.2.4 Techniques to improve laser induced forward transfer

LIFT has been used as the promising alternative to these techniques. Bohandy et al, 1986 [3] demonstrated that the transfer of film from donor substrate to acceptor substrate is due to the thermal ablation of the source film. The transfer of the thin film occurred when the thin film reached boiling temperature. The propulsion to the material is provided by the hot vapor which trapped between the source film and the donor substrate. This demonstration was supported by the experimental and theoretical model by Adrian et al, 1987 [17]. Willis et. al, 2005[28] also shows that the transfer of micro and nano-droplets can be done by careful control of melting of the donor film. The above studies show that the heating of donor film is necessary for forward transfer. Because of this, LIFT is not a suitable technique for sensitive materials. Absorption of laser energy in such materials may cause fracture to the transfer film. Some other problems are quite obvious in LIFT. For example, precoated metal film on a transparent support is required and usually produced with an expensive and sophisticated vacuum-deposition process. To address these challenges, many techniques have been developed to improve LIFT technique.

Some of these popular techniques are MAPLE-DW (Matrix assisted pulsed laser evaporation-direct write [29], laser induce thermal imaging [30], and dynamic release layer [31] .The use of femtosecond lasers in LIFT [32] has made this technique a definite topic of interest for its applicability to manufacturing. These techniques are listed and discussed in the following sections.

1. MAPLE – DW (Matrix assisted pulse laser evaporation-Direct write).
2. Dynamic release layer transfer.
3. Hydrogen assisted Laser induced forward transfer.
4. Laser induced thermal imaging.

1.2.4.1 Matrix assisted pulse laser evaporation – Direct Write

The matrix assisted pulse laser evaporation technique is a combination of LIFT and MAPLE techniques [33]. Matrix assisted pulse laser evaporation (MAPLE) is an alternative to Pulse laser deposition (PLD) technique [34]. MAPLE is a laser-assisted, vacuum deposition technique. It is used for the deposition of ultra-thin, uniform films and highly functionalized polymeric molecules, which cannot be transferred by using traditional PLD. In MAPLE, the material to be deposited is mixed in a particulate form into a solvent matrix material. The mixture is coated or frozen to a support substrate to act as a target. A focused laser beam is used to evaporate the matrix material and thin film is released and collected at acceptor substrate. MAPLE technique offers a number of advantages over conventional polymer deposition techniques, including the ability to precisely and accurately coat a relatively large or small targeted area with an ultra-thin and uniform coating with sub monolayer thickness control. Conventional pulsed laser ablation

techniques can be utilized for coating a limited number of polymers, but for highly functionalized materials the native polymer structure is almost completely lost in the process. But, using MAPLE, deposition of even highly functionalized polymeric materials is achieved with a little effect on the intrinsic polymer structure.

In MAPLE-DW, MAPLE and LIFT techniques are combined together to produce micro structures of sensitive materials. The material to be deposited is mixed with the matrix materials and coated onto the transparent donor substrate as a thin film. A laser of sufficient energy is focused thin film coated on the transparent substrate. When the laser strikes the film, a fraction of the polymer decomposes into volatile byproducts [35] (A. Pique 1999). Rapid evaporation of the matrix happens and releases the thin film. Figure 1.4 illustrates MAPLE-DW technique. MAPLE-DW technique is useful to transfer sensitive materials, because in this technique the laser energy is always kept below the threshold energy of material to be transferred. Due to low laser energy only the matrix material gets evaporated and the mechanical and physical properties of donor thin film remain same.

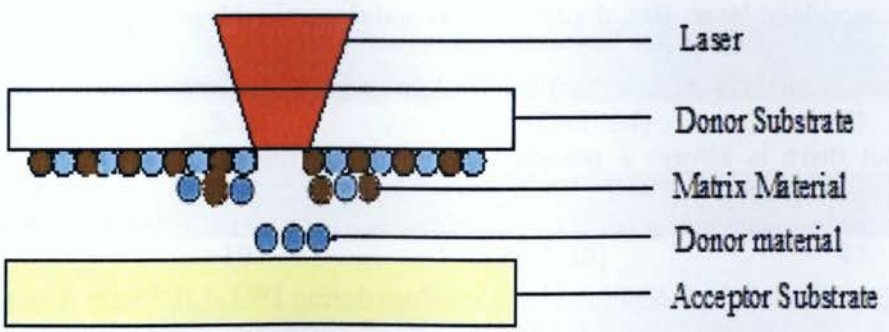

Figure1.4: Matrix assisted pulse laser evaporation-direct write (MAPLE-DW)

There are some other techniques available for the transfer of various materials from one substrate to the other without direct ablation of the material. There is another technique known as Hydrogen- Assisted Laser Induced Forward Transfer, in which hydrogenated thin film of the material to be transferred is irradiated with the help of laser (D. Toet et. al. 1999) [36]. The transfer of the material comes from the explosion of the hydrogen, when the hydrogenated thin film irradiates by laser. The material is transferred from donor substrate to acceptor substrate in the molten form.

1.2.4.2 Dynamic Release Layer Transfer:

There is another approach in which a sacrificial layer is inserted between the carrier and the donor. The purpose of sacrificial layer is to protect the donor layer during LIFT. This sacrificial layer is exposed to the laser and provides enough propulsion or driving force to the donor material. LIFT with a sacrificial layer was referred to as LIFT with dynamic release layer.

This technique is widely used for hard materials e.g. metals and ceramics and soft e.g. polymers and liquids without damaging them. In this technique there is no need to combine donor material with the sacrificial layer. But, donor material and dynamic release layer should be compatible to each other. In other words, it must be possible to grow donor material on the dynamic release layer. But there is always a possibility of dynamic release layer residue along with donor material on the acceptor substrate. Thin films have been used for the dynamic release layer applications. Researchers observed DRL residues during DRL-LIFT with donor material [37].

1.2.4.3 Laser Induced Thermal Imaging (LITI):

Laser induced thermal imaging technique is a forward transfer technique especially for the printing of conducting polymers [38]. As in case of DRL-LIFT, sacrificial layer gets ablated but in LITI, this sacrificial layer is not ablated but instead is designed to absorb the laser and heat up sufficiently to decompose the surrounding organics into gaseous fragments to provide the required thrust. When target (donor substrate with sacrificial layer and donor material) is removed or lift up, printed area remains stuck to the receiver substrate. In this technique there is no residue from the sacrificial layer because there is no ablation involved.

1.2.5 Overview of laser induced forward transfer work:

The investigations on LIFT are listed in the following table.

Material transferred	Feature size (μm)	Laser Type and wavelength (λ nm)	Reference #
Cu	50-70	Excimer	3
Ag	15-50	Frequency doubled YAG (532)	39
Ti, Ge/Se		Ruby (694)	40
W	5-10	Nd: YAG (1064)	41
Pd	150	ArF,KrF (193, 248)	42
Diamond	10	KrF (248)	43
Al		Nd: YAG (1064)	4
Al		Ti: sapphire (1053)	44
Au, Al	1-5	KrF (248)	45

Al, Ni	1-25	Nd: YAG (1064)	46,47
Al	5	(785, 45 fs)	48
Au/Sn	30	Ti: sapph (775)	49
Au	1	Ti:sapphire (800)	50
Au		Dye Laser (440)	51
Au	2-4	Ti: sapphire (400)	26
Au, Ni	150	KrF (248)	52
In_2O_3		dye laser (248)	53
$FeSi_2$	0.5	KrF (248)	54
Cu	1.5	(775, 150fs)	32
Pt,Cr	0.7-5	KrF (248)	55
Ni	150	KrF (248, 30ns)	56

Table 1.1: Overview of laser induced forward transfer work

1.3 Objectives of the present work

Even though laser induced forward transfer has become popular for material transfer. But, the material to be transferred needs to be coated on a transparent substrate and thin films coated on transparent substrate can only be transferred. In other words, the material transfer is efficient only when the coating thickness is of the order of microns (i.e. in the form of thin films). The main objective of this thesis is to investigate first time a reverse transfer technique in which material can be transferred from bulk material. Also, to investigate a material deposition

technique in which materials can be deposited on transparent substrate, due to high demand of deposition of various materials on quartz, in preparation of chemical and biological sensors, manufacturing of multilayer structures, formation of transparent ohmic contacts, templates for the design of nanoporous material and masks for non-lithographic patterning. Also, to optimize the various processing parameters like pulse width, scanning speed and pulse energy used in laser induced reverse transfer for material deposition.

1.3.1 Laser Induced Reverse Transfer (LIRT)

Laser induced reverse transfer can be divided into three steps as shown in Figure 1.5. First, the laser passes through transparent acceptor substrate and ablates the donor substrate, and then it transfers the material onto the acceptor substrate through plasma plume. The main advantages of LIRT over LIFT are, it uses less energy to ablate the donor substrate to obtain very small feature sizes, it allows to ablate only the section necessary for the transfer. On the other hand, in case of LIFT, the whole thin film is transferred [26]. The schematic comparison of LIFT and LIRT is presented in Figure 1.5.

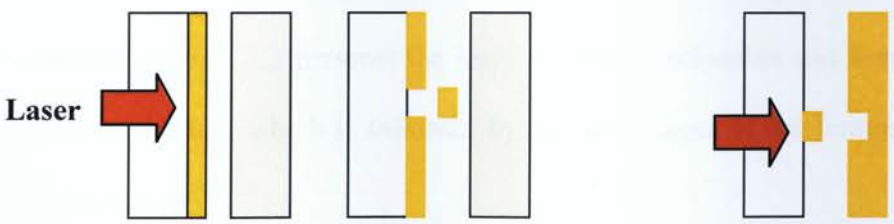

Figure1.5: Schematic shows the difference between LIFT and LIRT

Laser Induced Reverse Transfer is performed first time using a femtosecond laser system (515 nm wavelength) with repetition rates 13 MHz, 26 MHz, pulse widths 214.29 fs, 428.57 fs,

714.29 fs, 1428.6 fs and 3571.4 fs and scanning speeds 1000 μm/s, 2500 μm/s, 5000 μm/s, 7500 μm/s and 10000 μm/s.

1.4 Scope of this work

In chapter 1, a detailed explanation of laser induced forward transfer has been presented. Chapter 2 covers a brief introduction to laser and femtosecond laser-material interaction. In chapter 3 the details of experimental setup and laser parameters used are presented. The experimental results and discussion are presented in chapters 4 and 5. In chapter 4 the mechanisms underlying reverse material transfer is presented. Also the influence of pulse energy and scan speed on deposition thickness is presented. Chapter 5 covers the effect of pulse width and scan speed on ablation threshold and deposition thickness. In Chapter 6 conclusions and future work are presented.

monochromatic, directional and coherent. Monochromatic means that all of the light produced by the laser is of a single wavelength. White light is a combination of all visible wavelengths (400 - 700 nm). Directional means that the beam of light has very low divergence. Light from conventional sources, such as a light bulb diverges, spreading in all directions. The intensity may be large at the source, but it decreases rapidly as an observer moves away from the source.

2.1.1. Types of lasers

The obstacles to create a working laser after the invention of MASER were a lot. In order to have lasers at all wavelengths many researchers were working to find an appropriate active medium and excitation technique. Depending on the type of active medium used, lasers can be classified into solid, gas and liquid lasers. Theodore Maiman was successful in inventing the first solid state ruby laser on May 16, 1960. The amplifying medium in Mainman's laser was a ruby crystal with silvered ends placed inside a spring-shaped flash-lamp used for excitation. Most solid state lasers are constructed by doping a rare earth element or metallic element into a variety of host materials. The most common host materials are $Y_3A_{l5}O_{12}$ (YAG), $LiYF_4$ (YLF) and amorphous glass. The Nd:YAG and Nd:YLF lasers are the most common solid state lasers in industry. After the Maiman's laser, Ali Javan, William Bennet, and Donald Herriot made the first gas laser using helium and neon gas. This type of laser (He-Ne laser) became the dominant laser for 20 years until less expensive semiconductor lasers took over in the mid 80's. The helium-neon laser is used for various applications like reading UPC (universal product codes), surveying equipment, etc. In helium-neon laser the lasing action is initiated by electric discharge rather than a flash-lamp. Then, C. Kumar N. Patel start working with carbon dioxide (published 1964) and carbon monoxide lasers which they mixed with nitrogen, helium and water to fine tune the laser

714.29 fs, 1428.6 fs and 3571.4 fs and scanning speeds 1000 μm/s, 2500 μm/s, 5000 μm/s, 7500 μm/s and 10000 μm/s.

1.4 Scope of this work

In chapter 1, a detailed explanation of laser induced forward transfer has been presented. Chapter 2 covers a brief introduction to laser and femtosecond laser-material interaction. In chapter 3 the details of experimental setup and laser parameters used are presented. The experimental results and discussion are presented in chapters 4 and 5. In chapter 4 the mechanisms underlying reverse material transfer is presented. Also the influence of pulse energy and scan speed on deposition thickness is presented. Chapter 5 covers the effect of pulse width and scan speed on ablation threshold and deposition thickness. In Chapter 6 conclusions and future work are presented.

CHAPTER 2 - FUNDAMENTALS OF LASER-MATERIAL INTERACTIONS

The main aim of this study was to investigate first time the LIRT process with femtosecond duration laser pulses. The benefits of using femtosecond pulses for various material processing applications are well known. In particular, they are well suited for microfabrication. This is due to the fact that femtosecond pulses do not interact with the ejected material, thus avoiding complicated secondary laser-material interactions. Further, the material reaches extreme temperature and cools down in a very short time. This leads to material states which cannot be produced using longer pulses of comparable energy. The fast cooling also results in minimal heat accumulation and a small heat affected zone. For these reasons, the material transfer process is efficient with femtosecond laser pulses. In order to use this technique effectively for micro-fabrication, it is necessary to have a better understanding of femtosecond laser material interactions.

This chapter mainly consists of two sections. Section 2.1 covers an introduction to laser and laser material interaction. Section 2.2 presents the laser ablation mechanism and femtosecond laser ablation material interaction, which is followed by the advantages of the femtosecond laser in material transfer process.

2.1 Introduction to lasers

Laser material processing is an intensive research topic since the invention of laser in the year 1960. Nowadays, laser radiation is used as an efficient and qualified tool in many industrial processes such as cutting, welding, surface hardening, micromachining of ceramic and polymers, and micro-drilling. LASER is an acronym which stands for Light Amplification by Stimulated

Emission of Radiation. Stimulated emission was first suggested by Albert Einstein in the year 1917. The precursor to the LASER was (Microwave amplification by stimulated emission of radiation) MASER. First MASER was made in the year 1954 by Charles H. Townes. Soon after masers became a reality, researchers began to look at the possibility of stimulated emission in other regions of the electromagnetic spectrum. Townes and Schawlow published first detailed proposal of optical maser in 1957.A laser basically consists of three parts: a resonant optical cavity called the optical resonator, a laser gain medium (also called active laser medium) and a pump source to excite the atoms or molecules in the active medium. Electrons in the atoms of active medium normally reside in a steady-state lower energy level. When energy is added (pumping) to the atoms or molecules of active medium, majority of electrons are excited to a higher energy level, a phenomenon known as population inversion. This is an unstable condition for these electrons. They will stay in this level for a short time and then decay back to their original energy level. The decay occurs in two ways: spontaneous decay - the electrons simply fall to their ground level while emitting randomly directed photons; and stimulated decay - the photons from spontaneous decaying electrons strike other excited electrons which causes them to fall to their ground state. This stimulated transition will release energy in the form of photons of radiation that travel in phase at same wavelength and in same direction as the incident photon. If the direction is parallel to the optical axis, the emitted photons travel back and forth in the optical cavity through the active medium between the totally reflecting mirror and the partially reflecting mirror. The light energy is amplified in this manner until sufficient energy is built up for a burst of laser radiation to be transmitted through the partially reflecting mirror.

Laser generates a beam of very intense radiation. The major difference between laser radiation and light generated by white light sources (such as a light bulb) is that laser radiation is

monochromatic, directional and coherent. Monochromatic means that all of the light produced by the laser is of a single wavelength. White light is a combination of all visible wavelengths (400 - 700 nm). Directional means that the beam of light has very low divergence. Light from conventional sources, such as a light bulb diverges, spreading in all directions. The intensity may be large at the source, but it decreases rapidly as an observer moves away from the source.

2.1.1. Types of lasers

The obstacles to create a working laser after the invention of MASER were a lot. In order to have lasers at all wavelengths many researchers were working to find an appropriate active medium and excitation technique. Depending on the type of active medium used, lasers can be classified into solid, gas and liquid lasers. Theodore Maiman was successful in inventing the first solid state ruby laser on May 16, 1960. The amplifying medium in Mainman's laser was a ruby crystal with silvered ends placed inside a spring-shaped flash-lamp used for excitation. Most solid state lasers are constructed by doping a rare earth element or metallic element into a variety of host materials. The most common host materials are $Y_3A_{l5}O_{12}$ (YAG), $LiYF_4$ (YLF) and amorphous glass. The Nd:YAG and Nd:YLF lasers are the most common solid state lasers in industry. After the Maiman's laser, Ali Javan, William Bennet, and Donald Herriot made the first gas laser using helium and neon gas. This type of laser (He-Ne laser) became the dominant laser for 20 years until less expensive semiconductor lasers took over in the mid 80's. The helium-neon laser is used for various applications like reading UPC (universal product codes), surveying equipment, etc. In helium-neon laser the lasing action is initiated by electric discharge rather than a flash-lamp. Then, C. Kumar N. Patel start working with carbon dioxide (published 1964) and carbon monoxide lasers which they mixed with nitrogen, helium and water to fine tune the laser

properties and got success in making first high powered gas lasers. After high powered gas lasers, Earl Bell invented ion laser by placing mercury ions in helium to create lasing action (published 1964). Although the mercury ion laser has never seen with many applications, it was a direct predecessor to the argon-ion laser developed by William Bridges. The gas ion lasers then led to the development of metal vapor lasers by many researchers who worked with different metal vapors. Then George C. Pementel invented chemical lasers in the year 1965. These lasers are powered by chemical reaction and can achieve high powers in continuous operation. In Deuterium fluoride laser (3800 nm) the reaction is due to combination of deuterium gas with combustion products of ethylene in nitrogen trifluoride. After chemical lasers, excimer laser was invented in the year 1970 by Nikolai Basov, using a xenon dimer (Xe_2) excited by an electron beam to give stimulated emission at 172 nm wavelength. An excimer laser typically uses a combination of an inert gas (argon, krypton, or xenon) and a reactive gas like fluorine or chlorine. Upon the appropriate conditions of electrical stimulation, a pseudo-molecule called an excimer is created and gives rise to laser radiation in ultraviolet range. Efficient use of lasers for precise material processing is difficult to understand without thorough knowledge of fundamental physics governing the interaction of laser radiation with materials.

2.2 Interaction of laser radiation with materials

The effects that can be observed when laser radiation propagates through a medium are reflection, absorption, transmission and scattering, all of which depend on the properties of the medium for the specific radiation wavelength.

2.2.1 Absorption and ionization

The process of absorption is an important aspect to consider for materials processing applications. The absorption takes place through the excitation of valance electrons. There is a tendency for bond breaking to occur when the excitation energy surpasses the bonding energy of material [57]. Short (less than 1 ps) and longer (or continuous wave light) laser pulses interacts differently with materials. Under short pulse laser irradiation the energy deposition occurs on a timescale that is shorter compared to the electron-phonon relaxation time. The electrons absorb all the energy, leaving none for the remaining ions. These electrons rapidly transfer absorbed energy after the laser pulse by heat diffusion and by heat transfer to ions (phonons) but before the start of hydrodynamic expansion. The transfer process is controlled by electron phonon relaxation time, which is strongly material dependent and continues for several picoseconds until thermal equilibrium is reached. Short laser pulses, even those of relatively moderate energy, have a high enough intensity to propel nonlinear absorption processes in materials. This is not necessarily the case for longer pulses.

2.2.1.1 Linear absorption

The linear absorption of radiation from pulsed laser is similar to that of absorption from CW laser radiation. This holds true for both non-metallic and metallic materials. In non-metallic materials, there is an energy gap (i.e. bandgap) between the valence band and conduction band. This occurs because the highest energy level in valence band is occupied by an electron while the lowest energy level in conduction band is empty. In order to promote electrons from valence band to conduction band, the photon energy must surpass the bandgap energy so that light can be absorbed by non-metallic material. In the case of metals, the conduction band is partly occupied. This creates unoccupied energy levels at a slightly higher energy level than those that are

occupied. Due to this structure, photons can be absorbed through an interaction process called free-carrier absorption. This process causes an electron to gain energy by absorbing a photon, and then it gains momentum through an interaction with another phonon to shift to a higher conduction band level. For insulators, interband transitions between the conduction and higher bands can occur. With the use of linear absorption, there is great possibility for material ablation to occur if a sufficient amount of laser energy is accumulated into the surface of the target material.

2.2.1.2 Nonlinear absorption

Some materials are transparent to the laser wavelength and have difficulty in absorbing laser energy. The problem arises because in linear absorption a single photon of light does not possess sufficient energy to excite an electron from the valence band to the conduction band. A nonlinear process must be used to overcome this obstacle. The nonlinear process of absorption has the ability to ablate or permanently change the structure of the material if sufficient laser energy is deposited. Nonlinear absorption occurs when the absorption is approximated as a nonlinear function of the laser light intensity. Since the absorption is nonlinear, it can be restricted to the bulk of a sample by closely focusing the laser beam inside the sample. In turn, it produces much higher laser light intensity inside the material than at surface.

Nonlinear absorption can be explained with two types of nonlinear excitation methods such as photo ionization and avalanche ionization. In photo ionization, a laser radiation excites the electrons directly from the valence to conduction band. Depending on the laser repetition frequency and intensity, photo ionization can be classified into multi photon ionization and tunneling ionization.

In multi photon ionization, there is a simultaneous absorption of multiple photons by an electron. This occurs at higher laser repetition frequencies, but not higher than that of linear absorption. The sum of the energy of all the photons absorbed must surpass the bandgap energy. In tunneling ionization, the laser's electric field restricts the potential that joins a valence electron to its parent atom. This, in turn allows the electron to leave the field and become a free electron. This type of nonlinear ionization is led by powerful laser fields and low laser repetition frequencies. The schematic of avalanche and multiphoton ionization is presented in Figure. 2.1.

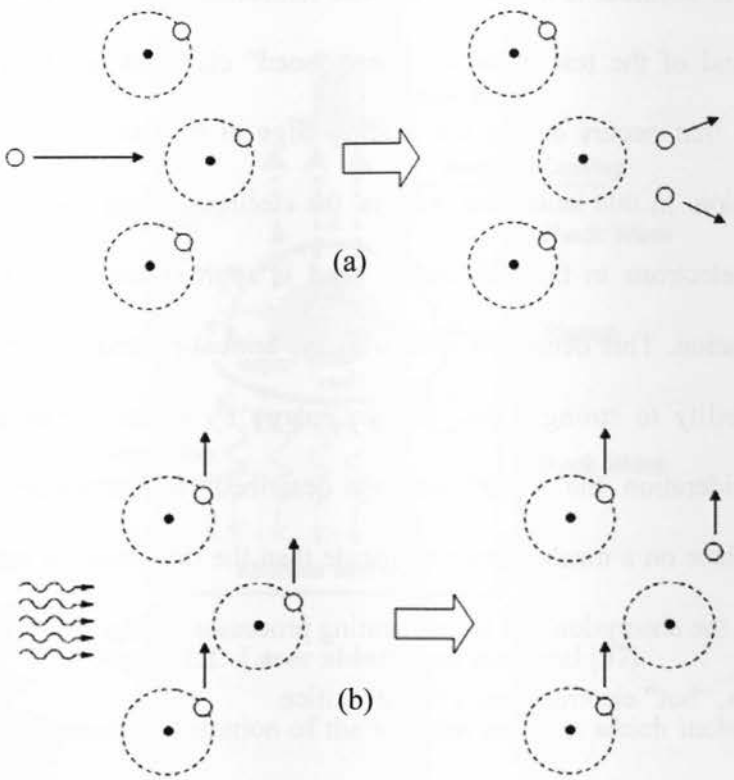

Figure2.1: Schematic of electron avalanche by (a) collision impact ionization (b) multiphoton ionization process [58]

Avalanche ionization uses free-carrier absorption by an electron in the conduction band of the material which is then preceded by impact ionization. An electron in the conduction band absorbs several laser photons in a particular order until its energy surpasses the conduction band minimum energy (which is greater than the bandgap energy). Then a collision occurs between the first electron and a second electron where the second electron leaves the atom to become ionized. This leads to two electrons at the conduction band minimum. The electron density in the conduction band continues to increase exponentially as long as the laser field is present. With the presence of the laser radiation, this process repeats itself continuously.

An important fact to consider is that the avalanche ionization requires a few "seed" electrons in the conduction band of the test material. These "seed" electrons are provided by the photo ionization process that occurs during the leading edge of the laser pulse for laser pulses of femtosecond duration. In this ionization process, the electron density increases until the plasma frequency of the electrons in the conduction band is approximated by the frequency of the incident laser radiation. This density is known as the critical plasma density. The high density plasma has the ability to strongly absorb laser energy by a free-carrier absorption process. Taking into consideration the absorption just described, for ultrashort pulse widths, the absorption takes place on a much shorter timescale than the timescale for energy transfer to the lattice, decoupling the absorption and lattice heating processes. At the end of the laser pulse, only two entities remain, "hot" electrons and a "cold" lattice.

2.3 Pulsed laser ablation

Ablation, in the broadest sense, is removal of material because of the incident light. In most metals and glasses/crystals, the removal is by vaporization of material due to heat. The processes

during laser ablation can be briefly summarized as follows. Upon irradiation of the laser beam on the surface, the heat waves penetrate into the bulk of the substrate, generating vapor and melt. As more heat is supplied, due to the rapid heating and heating-induced instability, evaporated particles are explosively ejected from the surface. The ejection of the particles from surface induced by irradiation with a high intensity laser beam leads to the formation of a cloud of ablated material known as plasma or plume, moving rapidly away from the surface. This cloud consists of excited electrons and ions. The expansion of plume and the rapid ejection of removed material create shockwaves as shown in Figure 2.2. Fractures might appear on the surface as a result of the propagation of the large shock-wave pressure-induced and thermal-induced stress.

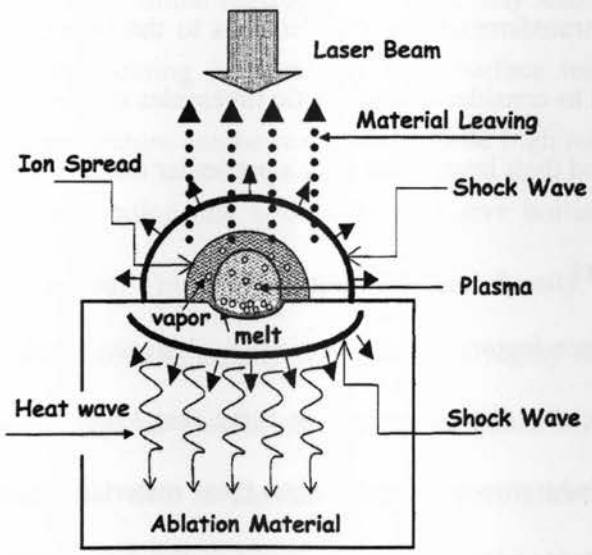

Figure2.2: Laser ablation of material [57]

Figure 2.2 shows a schematic illustration of the ablation process, which includes heat transport, plasma, shock wave, and vapor and melt formation. For nanosecond or longer pulses, the physical process of laser-matter interaction is characterized by thermal diffusion and plasma absorption which results in the partitioning of laser energy between plasma and bulk material;

whereas for femtosecond or ultra short pulses, it is characterized by the formation of hot and dense plasma, plasma heating and then heat diffusion.

2.3.1 Energy relaxation

The laser radiation interacts mainly with the electronic states of valence and conduction bands. The laser pulse-width determines the amount of time it takes to deposit energy within these states. For very short laser pulses, the resultant energy distribution of electrons that occur at the end of the laser pulse may be non-thermal. In a very short time period (merely within a fraction of a picosecond) this non-thermal energy distribution will settle down to a Fermi-Dirac distribution. The deposited energy is restructured over a range of different energy states of the system (i.e. energy is transferred from the electrons to the lattice). As mentioned in previous sections, it is important to consider characteristic timescales of ultra short and longer laser pulses to thoroughly understand their interaction with a particular material or matter.

2.3.2 Heat transport

Heat transport in semiconductors and dielectrics is relatively small, since the electrons cannot escape the field due to the charge separation force that keeps the material neutral. There is greater heat diffusion and transport in metals than these materials. In metals, "cold" electrons are replaced by "hot" electrons moving into the target material from the neighboring region. With the use of ultrashort pulses, heat diffusion in metals is significantly reduced due to strong non-equilibrium interactions between electrons and the lattice. Ultrashort laser pulses are prove to be advantageous in that it reduces the heat affected zone (HAZ). Here, there is less molten material due to absence of liquid phase and less debris. Thermal defects (i.e. cracking, chipping and delaminated) can be significantly reduced due to the reduced HAZ.

2.3.3 The plasma

The ejection of particles from a surface induced by irradiation with a high intensity laser radiation leads to the formation of a cloud of ablated material. The cloud formed due to ablation is known as plasma plume and consists of excited or ground state neutrals, electrons and ions. The physical parameters in the plume such as the mass distribution, ion and atom velocity and the angular distribution of the plume species, play an important role in the production of thin films.[59, 60] (Hubler, 1992; Chrisey and Hubler, 1994). In particular, the thickness distribution in film deposition on a substrate is determined by the plume shape that has evolved during the expansion from the target surface to the substrate [61, 62] (Saegner, 1994; Schou, 2006). During the light absorption in the solid, the initial heating of the solid may lead to a strong evaporative ejection of material. Since the heating is extremely fast, surface temperature close to the thermodynamically critical temperature can be reached. At these high temperatures the material ejection may change from evaporation and boiling to explosive boiling, by which nano and micro particle can also be ejected. This high temperature and density leads to high pressure, which causes the plume front to expand rapidly with time in a highly forward-directed pattern. The characteristics of laser generated plasma depend on the material, the laser pulse width, wavelength and laser intensity as well as ambient conditions. Figure 2.3 shows a schematic visual of the plasma composition at a distance from the surface of the target area of the material. Expansion of plume is different in case of gas background than in vacuum or at atmospheric pressure. If the expansion takes place in the vacuum, the shape and velocity distribution in the plume will reach asymptotically constant values.

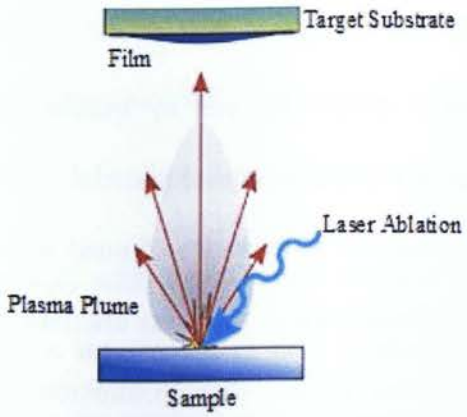

Figure2.3: Schematic illustration of Plasma plume

In case of background gas, the shape of the plume will be affected due to the presence of the background gas particles. At the first stage of the expansion the plasma plume shape is not much affected by the presence of ambient particles, due to the difference between the particle density in the plume and in the background gas. At later stage, ambient gas particles are pushed out from the volume occupied by the ablated material particles, on account of kinetic energy transfer during collisions between ablated material particles and background gas particles. Gas particles are compressed in a higher density region in the front of the plume which leads to a decrease in the velocity of ablated material particle velocities. Indeed, the instantaneous velocity of the leading edge of the plume at a delay of 1 μs and for a background pressure of 100 Pa is about 1.0 $\times$ 10^4 ms^{-1}, compared with a value of 1.6×10^4 ms^{-1} [63] obtained for the expansion under vacuum. Figure 2.4 shows images of plume in low-pressure background gas and in vacuum at different times after the vaporizing laser pulse. Researchers have proved that by monitoring the plume, quality and uniformity of thin films can be determined [64].

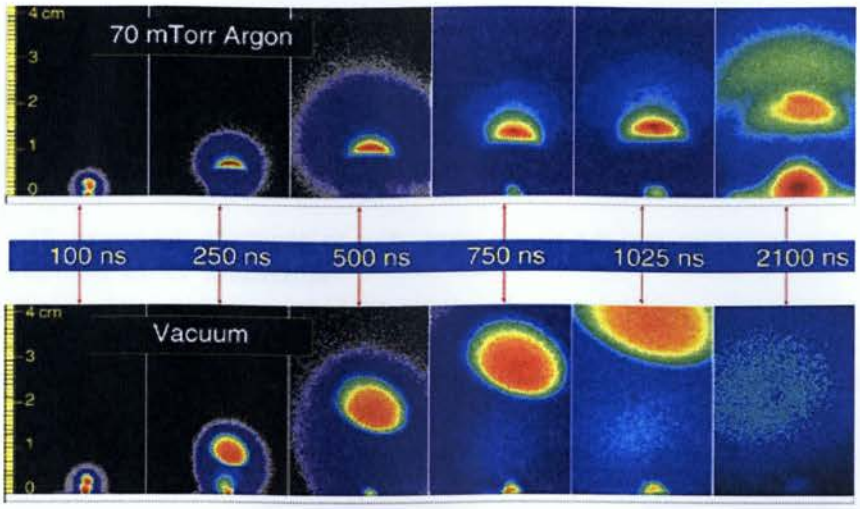

Figure2.4: Shape of Plume [64]

2.3.4 Shock wave

When the ambient environment for ablation is a gas, such as air, a shock wave is produced by the expansion of the plasma plume. The shock wave above the ablating material into the ambient gas is caused by the compression of the gas by the high velocity portion of the spreading of the ionized species, and by the high velocity expansion of the evaporated particles. A shock wave in the solid is caused by the generation and the expansion of the hot plasma, as well as by the subsequent heat conduction into the bulk. In the bulk of the ablating material, the shock wave overtakes when the heat conduction is slowed down by the occurrence of a phase transition.

When a shock wave propagates through the bulk of the solid target, a failure process called spallation or scabbing, can occur around the rear surface. The spallation is due to the crossing of two release waves: one of these rarefaction waves is generated by the unloading, starting from the front surface of the plate; the other one is the reflection of the first shock wave by the rear surface. The compressive stress wave interacts with the reflected tensile stress wave within the

target, and a sufficiently large tensile stress will lead to internal dynamic fracture. In reality, the propagation of the shock wave in the material is more complicated since the shock wave loses its energy as it propagates to create permanent strain. In general, at the beginning of the laser pulse, the shock pressure increases and the shock wave start to penetrate the target. The laser intensity determines the initial pressure of the shock wave, which determines its velocity. The thickness of the target and the shock (changing) velocity determine the travel time, and the travel time together with the initial velocity determine the shock attenuation and its pressure at the back surface.

2.4 Femtosecond laser material interaction

The physical process of laser-matter interaction is indeed very complicated and involves rich variety of different phenomenon especially when the pulse duration is on the order of femtoseconds or shorter can be drastically different from longer pulse regimes. The explanation for these differences is that the pulse duration is shorter than electron-ion coupling time in the target material. Many fundamental researches have been done to determine the physical mechanisms involved and their relative contributions in this complex and highly non equilibrium laser-matter interaction process [65- 67]. These mechanisms are not only of fundamental interest, but also are very important for engineering applications. There are vast varieties of laser parameters to choose from, including laser intensity, pulse width, wavelength and repetition rate etc. Therefore, understanding of the physical processes in laser-matter interaction becomes very crucial in choosing the optimal operating conditions. The ablation mechanism is dependent on the properties of the sample material. This section focuses on the fundamental physical mechanisms and characteristics of laser-matter interaction. Numerous researches have shown

that the mechanism of laser ablation is determined by pulse width [68-70]. Depending on the pulse width regimes, the mechanism can be thermal or non-thermal in nature. In the section, we will discuss the femtosecond laser ablation.

2.4.1. Femtosecond laser ablation

Ablation, in the broadest sense, is removal of material because of the incident light. In most metals and glasses/crystals, the removal is by vaporization of material due to heat. In polymers, the removal can be by photochemical changes which include a chemical dissolution of the polymer, similar to photolithography.

Due to the development in laser technology, laser is used as an efficient tool in many industrial processes. But, before invention of the femtosecond laser, the laser was not accepted as a universal tool in the micro-fabrication industry. Specially, for the precise micro-structuring of metallic materials, the use of nanosecond and microsecond laser is limited due to thermal and mechanical damage. These limitations have triggered the research activities to minimize the collateral damage and thermal diffusion out of the irradiated area by using femtosecond lasers. Metals, dielectrics, semiconductors and transparent materials can be easily micro-structured with femtosecond laser without any post-processing.

Many experiments and theoretical studies explain the presence of two different ablation mechanisms [71].

One is the thermal ablation and other is non-thermal ablation. If the pulse duration t_p is more than electron-phonon coupling time τ_{ei}, a material should go through the thermal melting. This is the reason, it is known as thermal ablation. On the other hand, if the pulse duration time is less

than that of the electron-ion coupling time. The ablation mechanism is called non-thermal ablation.

Because of the much faster energy deposition, ablation with femtosecond laser is totally different than that of the long pulse laser. In case of long pulse laser, the electrons and the lattice remain in the equilibrium and undergo thermal ablation. The duration of pulse is longer and heat diffuses out of the irradiated area and material expands. But in case of femtosecond laser, the electronic and ionic distribution is not in the thermal equilibrium. In femtosecond regime, the pulse duration is shorter than the electron-ion coupling relaxation time in the target material τ_{ei}. Reported values of electron-ion relaxation time is $\tau_{ei} \sim$ 1-10 ns [72, 73].

Initially, the femtosecond laser is absorbed by bound and free electrons inside the surface layer. Laser energy is absorbed firstly by electrons because of their mass is far less than that of the ion mass. After the absorption, heating of the free electrons and excitation of the material happens by inverse Bremsstralung. According to Inverse Bremsstralung principle, when energy in the form of photons is moving through a very small volume, the atoms in that volume become so excited that they stripped of their electrons and becoming ionized. Also at the absorption, the electrons exchange energy with each other by colliding. In other words, fast energy relaxation within the electron subsystem happens. Then the electron subsystem reaches the thermal equilibrium after tens of femto-seconds. If the laser irradiates the target, the electron subsystem continues to absorb the laser energy and its temperature increases continually. At the same time, the ion absorbs a little energy. The ion temperature is almost unchanged. It induces the tremendous difference of the temperature between the ion and the electron subsystem. Therefore, there are two different temperatures present. One is of the electron subsystems (T_e) and the other temperature is of the ion subsystem (T_i) within the target. This is the physical background of

building TTM (Two temperature model) in which the electron and the lattice are characterized by their temperatures. The corresponding laser ablation process is called non-equilibrium ablation (NEA). Now on the other hand, due to ion-electron interaction (electron-ion coupling), the temperature difference between the electron subsystem decreases gradually. After several picoseconds, two subsystem temperatures reach equilibrium. This kind of ablation is called thermal equilibrium ablation (TEA).

2.5 Advantages of femtosecond laser in material transfer

By using femtosecond pulses, smaller feature sizes can be obtained than using nanosecond pulses. In nanosecond regime because of the much larger heated volume, greater pulse energies are required to initiate the same phase changes. The higher pulse energies result in an overall larger heated area and more violent process, give rise to the crack formation and collateral damage typically with the long pulsed ablation. Conversely, femtosecond laser require only low pulse energies to vaporize and ablate the thin film. Due to smaller heat affected zone and smaller melted area in case of femtosecond pulses, the droplet size should be smaller. Also, less violent process happen, which shows that material.

2.6 Summary

Thorough knowledge of the fundamental physics governing laser matter interaction is important for efficient use of lasers for precise material processing. The complicated physical process of laser-matter interaction involves variety of different phenomenon. The ablation mechanism is dependent on the properties of the sample material along with the laser pulse width. For the nanosecond regime the primary mechanism for material removal is through the phase explosion of the metastable liquid. For this regime the ablation process is identified as a thermal process

creating heat affected zone, melt re-deposition, cracks and shock waves. On the contrary, in the femtosecond regime the primary ablation occurs via a direct solid-vapor transition. The heat diffusion into the target is negligible, which results in much localized ablation and precise machining of the sample without thermal damage to the surroundings. The significant difference between femtosecond and nanosecond laser-matter interaction in terms of transferring laser energy into thermal energy of the target is that electrons and ions are not in equilibrium during the laser pulse in the Femtosecond laser ablation case. This is because the electron-ion relaxation time, which is in the range of a few picoseconds to a few tens of picoseconds, and is much longer than the sub-picosecond pulse length.

CHAPTER 3 - EXPERIMENTAL DETAILS

In this chapter, an overview of the laser system and the experimental setup used for this study is presented. These experiments were conducted using a high power, high repetition rate femtosecond laser system in the Micro and Nano Fabrication Research Lab, Department of Mechanical and Industrial Engineering, Ryerson University, Toronto, Canada.

3.1 The femtosecond laser system

The experiments were carried out using a diode-pumped Yb-doped fiber oscillator/amplifier system capable of producing variable repetition rates of 200 kHz to 25 MHz with an average power output of 12 W at 2 MHz (Clark-MXR Inc. IMPULSE Series Ultrashort Pulse Laser) (Figure 3.1). The Yb-doped fiber-oscillator/fiber-amplifier design allows for the low noise performance of solid-state to be combined with high spatial mode quality of fiber lasers. The laser can produce pulses with duration between < 250 fs and 10 ps. The laser beam produced has a central wavelength of 1.03 μm. All major laser parameters such as pulse width, repetition rate and total beam power are computer controlled.

Figure3.1: The Laser System

3.2 The optical setup

The schematic of optical setup used is shown in Figure. 3.2. The laser beam from the system is expanded by a combination of plano-convex and plano-concave lenses of focal lengths 500 mm and150 mm respectively. A λ/2-wave plate is kept in between the two lenses to control the beam polarization before second harmonic (515 nm) conversion. The second harmonic generation from 1030 nm to 515 nm increases the efficiency and ease with which the micromachining of the features were carried out due to reduction in the order of multiphoton absorption [74].

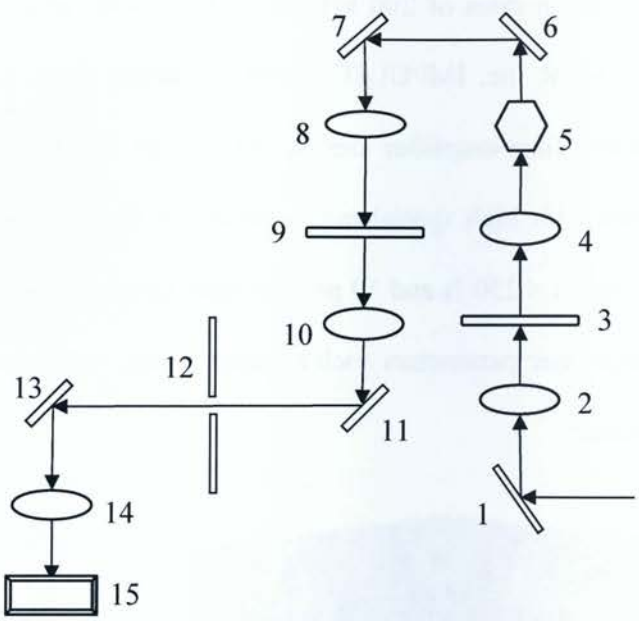

1. 1030 nm Mirror
2. F = 500 mm Convex Lens
3. 1030 nm λ/2 Waveplate
4. F= -150 mm Concave Lens
5. 515 nm Harmonic Generator
6. 515 nm Mirror
7. 515 nm Mirror
8. F= -75 mm Concave Lens
9. 515 nm λ/4 Waveplate
10. F = 300 mm Convex Lens
11. 515 nm Mirror
12. Diaphragm
13. Piezo Scanner
14. EFL = 12.478 mm Telecentric Lens
15. Sample and Sample Holder

Figure3.2: Schematic illustration of experimental setup

Three 515 nm mirrors are used to remove the 1030 nm wavelength component out of the beam. In addition, a plano-concave lens and a plano-convex lens of focal lengths 75 mm and 300 mm respectively are used to increase the beam diameter by 4 times to 8 mm. A λ/4-wave plate kept

in between the two optical lenses to ensure circular polarization of the beam. A diaphragm is used to correct the beam profile. The setup is presented in Figure 3.3.

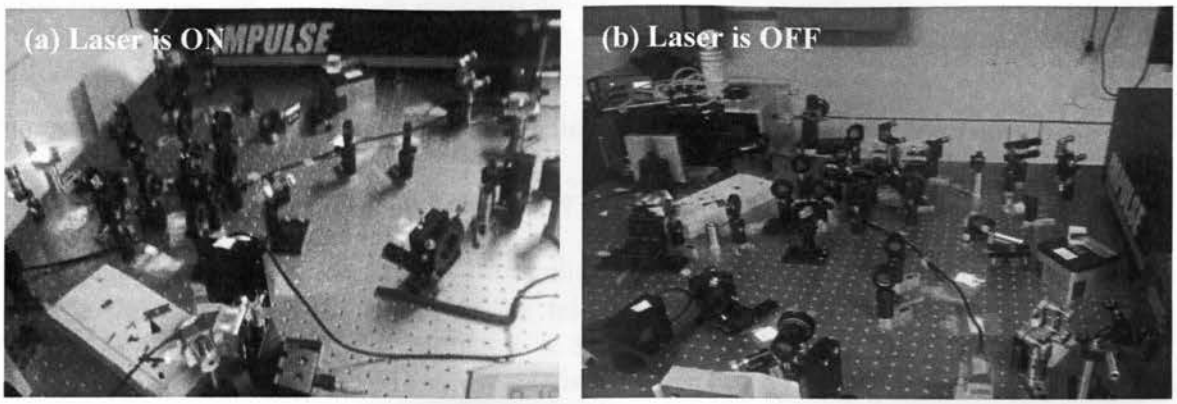

Figure3.3: Experimental setup in laboratory

Next, a unique piezo tip/tilt mirror is used to scan the beam onto the sample surface. The 16 mm dia, 2 mm thick mirror in piezo scanner consists of 2 fixed orthogonal axes with a common pivot point [75]. The common pivot eliminates the so-called pillow effect and hence the field distortion at image plane is eliminated and thus the compensation software to remove the distortion is not required. The novel lever design allows for an exceptional tip/tilt range of 50 mrad (~3°) with sub μrad resolution which translates to a beam deflection of up to 100 mrad (~6°) [75]. This parallel-kinematics design allows for a smaller package with faster response and better linearity with equal dynamics for both axes [75]. The mirror also incorporates zero friction, zero stiction flexure guides and has a high resonant frequency of 1 kHz [75]. This is critical for high repetition rate laser machining since precise pulse number control demands for high frequency beam steering. The frictionless guides and drives do not experience wear and tear which in turn leads to an exceptionally high level of reliability [75]. Finally, the beam is focused onto the sample surface using a telecentric lens with a 12.478 mm focal length [76].

The telecentric lens ensures that the laser hits the sample surface at 90° over the entire scanning field thus projecting the correct spot size and wall angle for our application [76].

3.3 Sample preparation

The specimens used for this study are gold coated silicon wafers. The wafers used are mounted on a two-axis (x and y) translation stage with a precision of 0.5 μm. The samples have a thin film (Gold) thickness of 3000 Å and a substrate (silicon) thickness of 250 μm. The substrates with transferred material are characterized using a scanning electron microscope (SEM). All experiments were carried out in ambient atmosphere. Various experiments have been conducted by transferring the gold (Au) on silicon (Si) wafer onto the quartz substrate in near contact, using the laser. The piezo-scanner controls the high speed laser beam positioning in the x-y plane. The laser beam passes through the transparent acceptor substrate and ablated the gold film. Pulse energies ranging between 8 nJ to 100 nJ is used for the material transfer. The laser is scanned at different speeds on the sample surface as discussed in chapter 4 and chapter 5, with repetition rates of 13 MHz and 26 MHz and pulse widths between 214.29 fs and 3.5 ps.

3.4 Parameters

For the deposition of materials, several basic parameters are mainly responsible for the achievable resolutions, processing speed and quality. These include laser fluence and spot size. These parameters and other aspects, pertaining to the experiments performed, will be discussed in detail in the subsequent sections.

3.4.1 Spot Size

Spot size, also known as the beam waist, is the minimum diameter of the Gaussian beam travelling in a free space. In order to find the size of the focused beam spot, a single spot can be

machined on a thin metal film, with pulse energy well above the material threshold. The size of the machined spot, measured using a Scanning Electron Microscope (SEM), gives the size of the focused beam spot. The theoretical laser machining spot diameter (D_0) was calculated from the equation given below [77].

$$D_0 \cong 1.27\frac{\lambda_0 f}{D}$$

Here, f is the effective focal length of the telecentric lens equal to 12.478 mm, λ_0 is the wavelength of the laser equal to 515 nm and D is the laser beam diameter equal to 8 mm. From this formula the theoretical spot size is calculated to be 1.02 μm in diameter. During the experiment the spot size may be bigger due to scatter and misalignment. Generally, smaller spot size results in higher laser fluency, which in return increases the smoothness and quality of deposition.

Also, pulse width and wavelength are the important parameters to be considered in the transfer of the material from one substrate to another. Shorter pulse width helps in achieving smaller feature sizes and lower threshold fluences.

3.5 Summary

In using short laser pulses as an alternative for silicon material transfer, laser parameters including wavelength, pulse energy and beam shape must be optimized to satisfy the requirements of specific tasks and to maximize the efficiency of laser power usage. Among other parameters of laser light-matter interaction, removal rate is an important performance factor that determines whether material transfer and deposition is appropriate for certain specific applications. Different multiple physical processes dominate under different laser operating

conditions and at different ablation stages. Through estimating the impact of each physical process, the laser parameters that affect the removal speed, deposition of the material and other quality factors can be determined.

CHAPTER 4 - EFFECT OF PLASMA PLUME ON DEPOSITION

In this chapter, the results of material transfer using laser induced reverse transfer are presented. This chapter is divided into four parts. Section 4.1 covers an introduction to the laser induced reverse transfer technique. Section 4.2 presents the experimental details and parameters used in this study. Section 4.3 covers the effect of fluence on the thickness of deposition. The last section 4.4 presents conclusions.

4.1 Introduction to laser induced reverse transfer

The laser induced reverse transfer (LIRT) technique has similarities to its laser induced forward transfer (LIFT) counterpart. In this study, LIRT has been performed first time using femtosecond laser of pulse width 214.29 fs, a repetition rate of 13 MHz and 515 nm wavelength with two different scan speeds of 4000 μm/s and 1000 μm/s. The main purpose of this study is to find a technique with which we can transfer material from a bulk material, not necessarily to be a thin film. Sometimes, its too hard to deposit a thin film. LIRT can be used wherever a thin film is difficult to deposit on a donor substrate. This is not the case for LIFT since thin films can only be transferred by using forward transfer. In LIRT, there is no need to transfer the whole film and the donor substrate can be of any material. But, in case of forward transfer, the donor substrate needs to be transparent to laser.

No doubt, the transparent acceptor substrate used in LIRT, limits its applications to some extent. But, this technique can be helpful in manufacturing of fluidic devices because of its simplicity and high throughput. Because of high demand of deposition of various materials on quartz, this

technique can be useful in preparation of chemical and biological sensors [78], manufacturing of multilayer structures [79, 80], formation of transparent ohmic contacts [81], templates for the design of nanoporous material [82] and masks for non-lithographic patterning [83].

In this work, we conduct first time an in-depth study on the Laser induced reverse transfer (LIRT) using high repetition rate femtosecond laser. Some interesting phenomena were observed and it was found that the profile of the deposition was closely related to the dynamics of the ablated plume and is presented in section 4.3.

4.2 Experimental detail and parameters of laser

Various experiments have been conducted under ambient conditions by transferring the gold (Au) onto the transparent quartz substrate in near contact, using femtosecond laser. The main source for femtosecond laser used in these particular experiments were from a direct-diode-pumped Yb-doped fiber oscillator/amplifier, which is capable of delivering a maximum output power of 20 W at a maximum repetition rate of 26 MHz, a maximum pulse width of 10 ps and wavelength of 1030 nm. A two-axis precision translation stage was used to locate the laser irradiation spot on the sample surfaces. A piezo-scanner was used for high speed laser beam positioning in the x-y plane. The average power of this laser varies between 0 W-20 W. The laser beam produced has a central wavelength of 1.03 μm. The laser beam diameter was expanded by a plano-convex lens of 500 mm focal length and a plano-concave lens of 150 mm focal length. A λ/2 wave-plate in between the two optical lenses was used to control the polarization of the beam before being converted to the second harmonic (515 nm) central wavelength using a harmonic generator. Small pulse energies of magnitudes between 8 to 100 nJ has been applied on the donor substrate. The laser beam has been scanned at two different scan speeds of 4000 μm/s and 1000

μm/s for gold film coated on silicon substrate (donor) with repetition rate of 13 MHz with pulse width of 214.29 fs. A quartz receiver/acceptor substrate was placed in close contact to the donor substrate on the movable X-Y stage. The donor and acceptor substrates move together on the X-Y stage. The acceptor quartz substrates were then examined under a scanning electron microscope (SEM).

Laser induced reverse transfer technique is basically consists of three steps. First, the laser passes through the transparent (acceptor) substrate and ablates donor substrate, and then it transfers the ablated material onto the acceptor substrate. Lastly, the ablated material is deposited onto the acceptor substrate.

On the other hand in case of forward transfer, laser first passes through transparent quartz (donor) substrate hitting thin film coated onto it and transfers the ablated material to acceptor substrate. In case of LIFT, the film should be thin coated onto transparent support. The deposition of thin films on transparent substrate requires highly precise procedures like pulse laser deposition and needs expensive equipments. Moreover, in order to initiate the deposition by LIFT, whole thickness of the donor layer needs to be completely ablated. On the contrary, LIRT does not demand for the whole film to be transferred. Bulk material can be used as donor itself. Also, thin film can be coated on any kind of support, it does not need to be transparent. Therefore, the sample preparation can be achieved by using simple and economical deposition methods like physical vapor deposition (PVD) and castings.

In LIRT, when laser passes through the acceptor substrate (quartz) and after hitting the target (any thickness) coated on the donor substrate, a plume in the direction opposite to the direction of the laser beam is obtained. Figure 4.1shows schematic illustrations of forward transfer (LIFT)

and Figure 4.2 (a, b) shows reverse transfer (LIRT) techniques. The results obtained are discussed in the following sections.

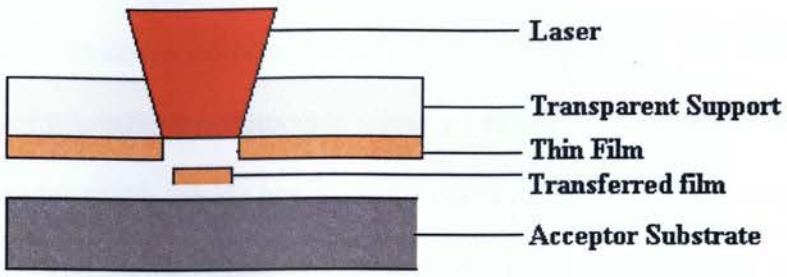

Figure4.1: Schematic illustration of Laser Induced Forward Transfer

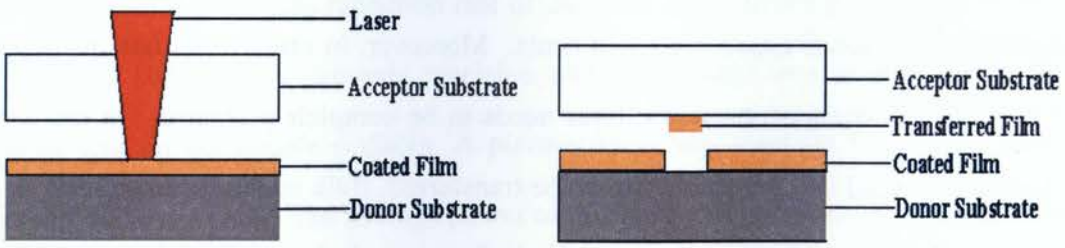

(a) (b)

Figure4.2: (a, b) Schematic illustration of Laser Induced Reverse Transfer

4.3 Effect of plasma plume and pulse energy on deposition

The pattern on the acceptor substrate depends on pulse energy of the laser beam. It was realized that no transfer of (gold) material on the acceptor substrate takes place at pulse energy magnitudes below 36 nJ. This is known as threshold energy, the energy required to start ablation. Deposition was measured from the SEM images at three different points and an average of the values was taken. These values came out to be within 5% variation and were plotted against the pulse width as shown in Figure 4.3. It shows the relationship between pulse energy and line width of deposition. It is obvious from Figure 4.3 that as the pulse energy increases, the line width of deposition increases. Deposition of gold has been obtained, with pulse energy between 40-82nJ. Above this value, no deposition was obtained. At high pulse energy, the vapor temperature is too high and the sticking coefficient decreases in magnitude. Therefore, at a very high pulse energy the transfer material does not stick to the acceptor substrate[26].

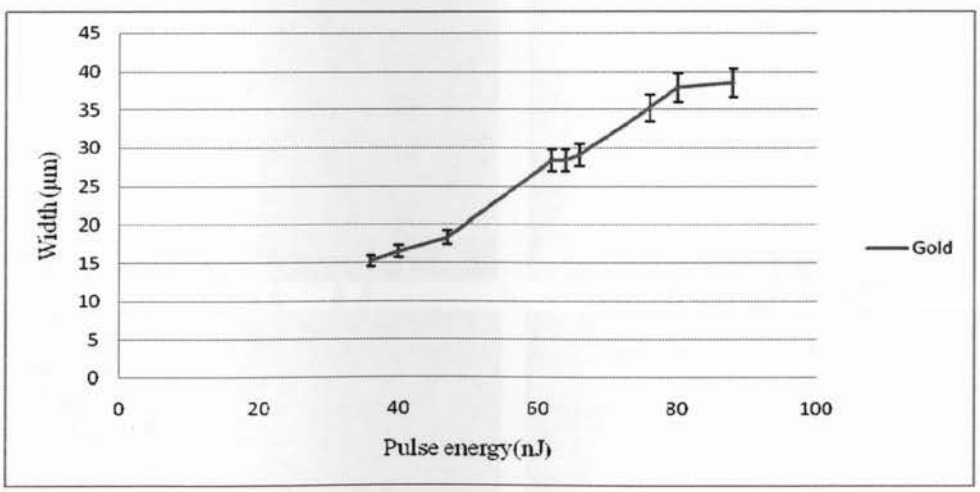

Figure4.3: Effect of pulse energy on thickness of deposition

On the other hand, with increase in scan speed, deposition width decreases as shown in Figure 4.4. This has been proved by many researchers [26], this is believed to be fact that at high scanning speed, the beam-material interaction time is not long enough to activate the surface fully and uniformly.

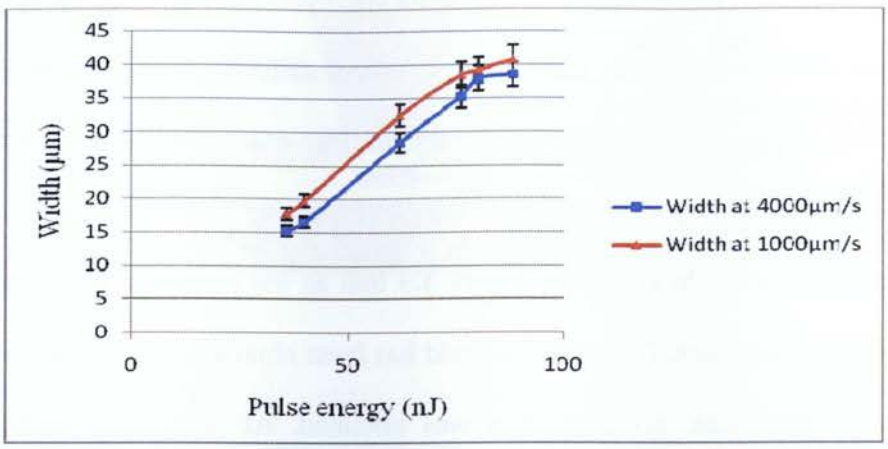

Figure4.4: Effect of scan speed on thickness of deposition

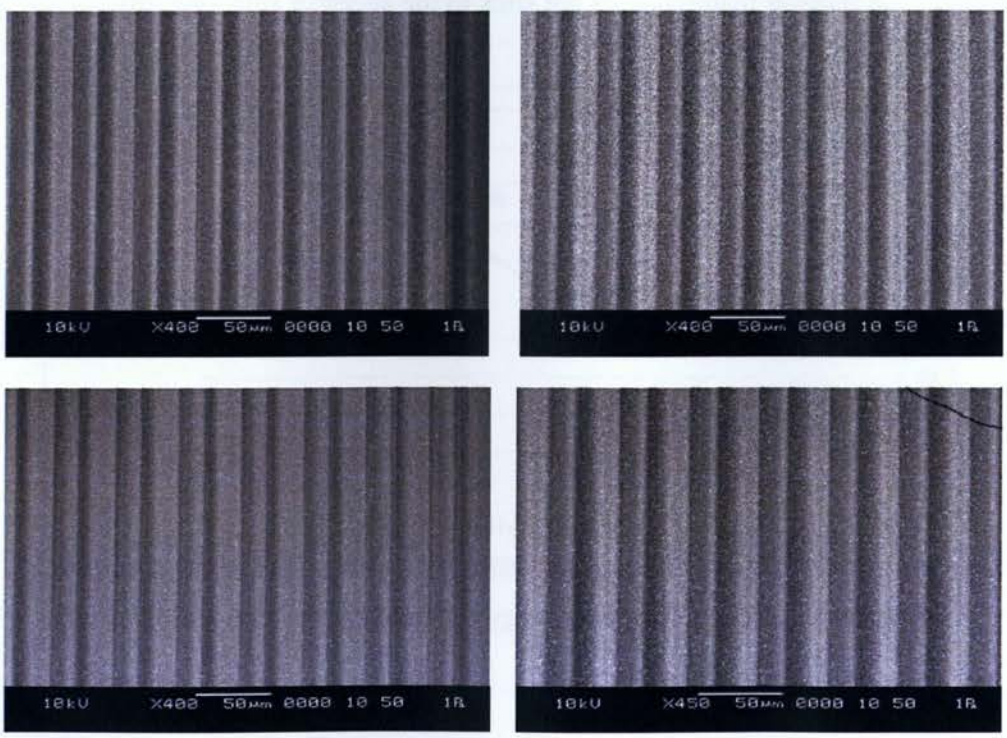

Figure 4.5: SEM photographs of gold samples

Some of the SEM photographs of gold sample have been shown in Figure 4.5

Figure 4.6 (a-c) shows schematic illustration of effect of pulse energy on the deposition and figure 4.7 (a) was the result obtained from SEM, and shows that solid lines were obtained with the pulse energy in the range of 36nJ to 40nJ. The thickness of line deposited at 40nJ was 16.34μm. The width of deposition obtained on acceptor substrate was 28.36μm at 62nJ. After 62 nJ, thickness at centre gets thinner, as shown in Figure 4.7 (b).The width of deposition obtained was 38.47μm with wider crests at 82nJ, as shown in Figure 4.7(c). The structure evolution of the deposited lines can be explained by the dynamic of the ablated plume.

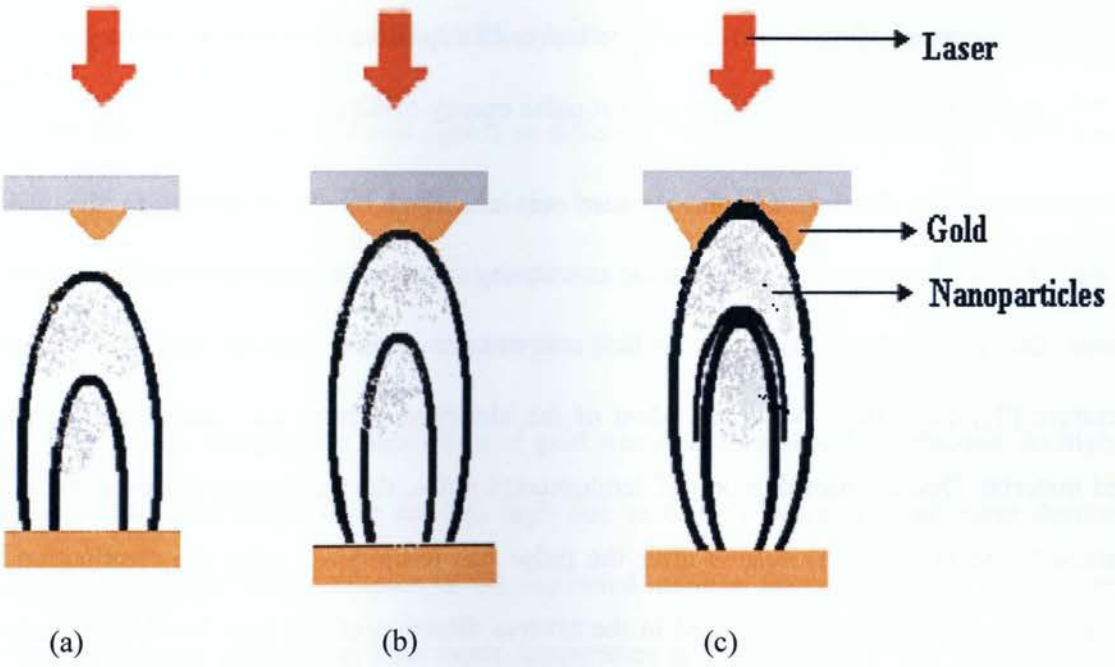

Figure 4.6: Schematic illustration of effect of plume of deposition

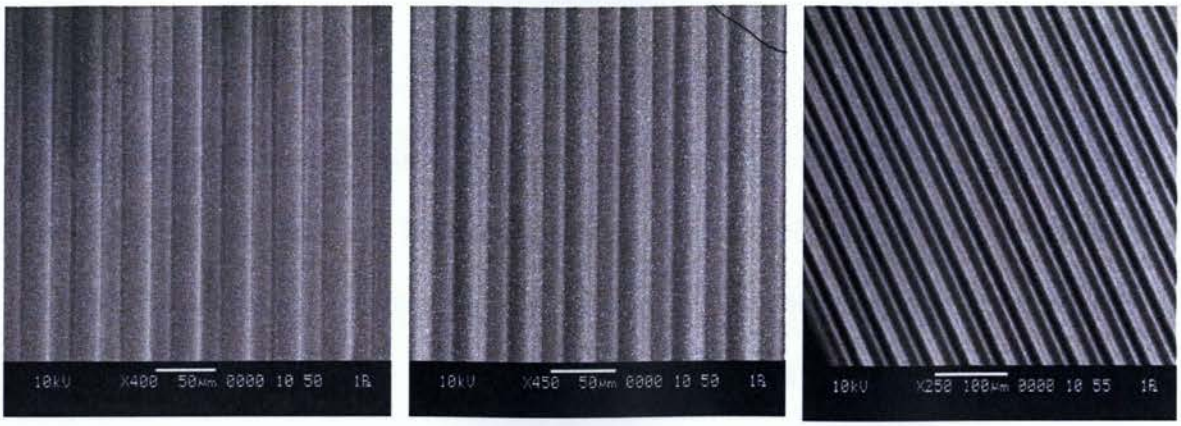

(a) (b) (c)

Figure 4.7: Effect of plume on deposition (SEM pictures)

Figure 4.7: Deposition of gold on the quartz substrate, 4.7(a) shows the SEM image of deposited gold at pulse energy of 40nJ, 4.7(b) shows the image of deposited gold at pulse energy of 62nJ and 4.7(c) shows the image of deposited gold at pulse energy of 82nJ.

Upon irradiation, the femtosecond laser pulse was absorbed by the electrons in the donor substrate. The fast heating of the target leads to a strong evaporation of the material in the form of plume. Due to this fast heating, the surface temperature close to thermodynamically critical temperature (T_c) can easily overcome. Most of the absorbed energy was carried off with the ejected material. Due to short duration of femtosecond pulse, the movement of the atoms from the lattice (solid gold target) ensued after the pulse has terminated. After the termination of femtosecond pulse, the plume expanded in the reverse direction of the laser beam propagation. The plume contains an atomic front and an ablated-particles front [84]. Atomic front consists of very fast moving electrons, atoms and ions moving at an average velocity in the order of 10^4m/s [84]. On the other hand, ablated-particles front has slow moving nanoparticles with average velocities in the order 10^2m/s [84]. This plume reaches very high temperatures of a few eV

because of the electron-atom collisions inside the atomic front. The higher laser fluences lead to faster propagation in space at a temperature of few eV. The slow ablated-particles in the plume hit the receiver substrate and gets deposit onto the acceptor substrate. At pulse energy just above the ablation threshold, the plume front is spherical. As the pulse energy increases, the front gets sharpened. Also, the plume length, atomic front velocity [85] and temperature of the atomic front increases with the increase in pulse energy.

As the pulse energy increases deposition width also increases as shown in Figure 4.3.The pulse separation time with using 13MHz repetition rate is ~ 0.7μs. The subsequent pulse with high temperature and faster propagation atoms, brushes the deposited material from the first pulse. This result in the crest formation observed at higher pulse energy. As the pulse energy reaches to 82nJ, the centre of deposited gold is totally wiped-off by atomic front of the next pulse.

The thickness of transfer material (gold) at different velocities (scan speed) of 1000 μm/s and 4000 μm/s at a 13 MHz repetition rate has also been examined and shown in Figure 4.4. It shows that the width of the transfer material decreases as the scan speed increases. This has been proved by researchers even for forward transfers [26].

For higher pulse energies, no deposition of gold was found on acceptor substrate. At high pulse energy values, the temperature are too high due to this the sticking coefficient decreases in magnitude and also the re-ablation of the deposited material take places. Due to the combined effects of reduced stickness at high vapor temperature and re-ablation of the deposited material, there is no deposition presents on the acceptor substrate at higher pulse energy.

From the above discussion, we can conclude that in order to obtain solid deposition, the pulse energy should be maintained just above the threshold energy in the range of 36 to 40nJ. Crest at

centre of the deposition presents when the pulse energy is in the range of 40 to 82nJ. Also, at high pulse energy above 82nJ, only traces of deposited material can obtained.

4.4 Summary

For the first time, LIRT was studied in detail using femtosecond laser and the evolution of deposited gold structure was analyzed. Solid deposition was obtained at energy just above threshold energy. Higher pulse energy creates crests and wiped off deposition at the center of deposited spot. LIRT may provide an alternative for applications that LIFT does not applicable or where thin film donor is difficult to process. Since LIRT allows for minimum transfer of the donor material because there is no requirement to transfer the whole donor thin film, high resolution deposition can be achieved. The structures obtained by only one shot of femtosecond laser pulses at 82nJ can be used as fluidic channels. The deposition of material on the transparent quartz substrate by using this simple, economical, high throughput technique can be very helpful in manufacturing of the fluidic devices.

CHAPTER 5 - EFFECT OF PULSE ENERGY, PULSE WIDTH AND SCAN SPEED ON LIRT

In this chapter, the results of gold deposition using five different scan speeds of 1000 μm/s, 2500 μm/s, 5000 μm/s, 7500 μm/s and 10,000 μm/s with pulse widths of 214.29 fs, 428.57 fs, 714.29 fs, 1428.60 fs and 3571.40 fs at a pulse repetition rate of 26 MHz are presented. Section 5.1 covers an introduction to ablation threshold. Section 5.2 presents the effect of pulse width on ablation threshold energy. Section 5.3 covers the effect of pulse energy and scanning speed of the laser on the thickness of deposition using a very high repetition rate of 26 MHz. Section 5.4 presents the effect of pulse width on the thickness of deposition.

5.1 Introduction

Ablation threshold energy also known as threshold fluence (energy/cm^2) is the minimum laser energy required to initiate material removal or can be defined as minimum energy necessary to break the bonds between molecules of the material. Ablation occurs when the fluence exceeds a certain threshold value, typical of a given material and it also depends on the laser pulse width. The mechanisms of material removal are strongly dependant on physical properties of the solid, pulse width and laser fluence [86-88]. With the increasing availability of ultra short laser pulses and their application in the field of material structuring or deposition/transfer, there is growing evidence of high precision, quality processing with femtosecond to picosecond laser pulses when compared to nanosecond or longer-laser pulses. Harzic and group (2005) compared ablation threshold and rates of steel, Cu and Al with femtosecond laser pulses at low and high energy densities with 80 MHz pulse repetition rate and found that ultrashort pulses offer several advantages over longer pulses. It is observed that the loss of ablation rate is associated with low

fluence of femtosecond pulses. This loss could be compensated using higher repetition rate lasers, which were not commercially available at that time [89]. Since ultra short laser pulses play a role in industrial materials deposition/transfer, it is desirable to understand the limitations in processing and parameters determining these limitations for various materials to decide an optimum laser system for a particular application. However quality of deposition/transfer is material and wavelength dependent and shorter laser pulse is not always better for the precision and controllable deposition. Investigation on femtosecond laser irradiation of materials by Korfiatis and group (2007) revealed the dependence of fluence thresholds on wavelength and pulse width, and found that the threshold fluence increases with pulse width. For an industrial material transfer, the question of using ultra short (fs) or short pulses (few ps) is open because of a higher simplicity of amplified picosecond laser systems and their better cost-effectiveness and reliability [90].

Despite intensive investigations and considerable progress achieved over the last two decades, the mechanisms of ultrashort laser material transfer are still an issue of much debate. Further material transfer using LIRT have been never investigated due to the non availability of high power and high repetition rate laser systems. In this section, the effect of laser pulse energy, pulse width and scan speed on reverse transfer of gold is presented. Gold coated silicon samples are irradiated with laser pulse widths 214.29 fs, 428.57 fs, 714.29 fs, 1428.60 fs and 3571.40 fs at 26 MHz repetition rate. Further the dependence of fluence thresholds on pulse width is also studied. The width of gold deposition on glass acceptor substrate was examined by scanning electron microscope (SEM).

5.2 Effect of pulse width and scan speed on ablation threshold

In laser ablation, feature size is determined by the maximum laser fluence, $ø_o$, which must exceed the threshold value to cause an irreversible change on the surface. As mentioned earlier, the threshold fluence, ø, depends on material and number of laser pulses, applied at each scanning point. For laser pulses with Gaussian intensity profile, the feature size D can be related to the maximum laser fluence $ø_0$ on the sample surface by [91]:

$$D^2 = 2\omega_0^2 \sqrt{\frac{\phi_0}{\phi_{th}}} \qquad \textit{(Equation 5.1)}$$

where ω_0 is the beam radius, $ø_o$ is maximum laser fluence and $ø_{th}$ is threshold fluence. The maximum laser fluence is related to the measured pulse energy E_{pulse} by [92]:

$$\phi_0 = \frac{2E_{pulse}}{\pi\omega_0^2} \qquad \text{(Equation 5.2)}$$

In order to find the threshold fluence of the gold coated silicon wafers used in the study, for each combination of pulse width and scan speed, laser power was recorded for the point at which ablation takes place. The threshold fluence values were plotted against laser pulse width, as shown in Figure 5.1.

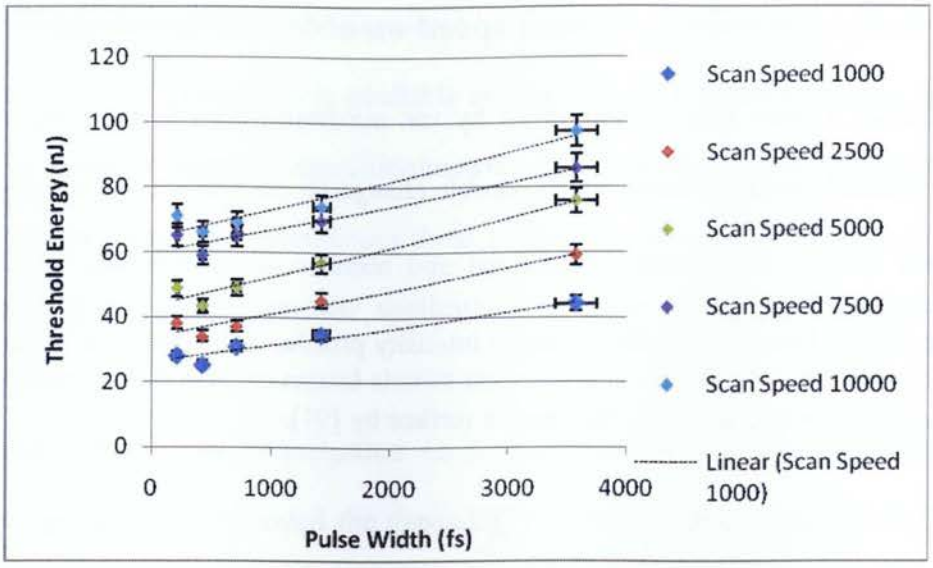

Figure5.1: Effect of pulse width on threshold energy

Dependence of ablation threshold fluence on the pulse width can be clearly observed from the plot of threshold fluence and pulse width. The threshold fluence is found to increase with the increase of pulse width from 429 fs to 3.5 ps. This trend of increase can be associated with the thermal diffusion of laser energy in the material at different pulse widths. The longer the pulse width, more time is available for heat to diffuse into the bulk before the vaporization stage is achieved. However, the rate of increase observed in the present study seems to be considerably small and hence threshold fluence can be considered to be nearly constant except for 429 fs pulse width where, a slight decrease in threshold is observed. This can be explained by the thermo-physical effects occurring in this range of pulse width which includes the finite velocity of the vapor front relative to the underlying material as well as the structure of thermal gradients at the surface where vapor is supported and deeper in the material where the bulk diffusion occurs [93]. The thermal gradient in the bulk and on surface will increase with the decrease in the pulse width. The finite velocity of the vapor front determines the relaxation of the near surface gradient

while the bulk diffusion determines the temperature profile in the bulk of the material. These two gradients together determine the amount of energy lost to the vaporization and to the bulk. Increase in the amount of energy drawn into the bulk will result in increase of the threshold values. Decrease in pulse width results in commensurate changes in the fraction of the pulse energy that is distributed among the solid, liquid and vapor phases, as the incoming pulse goes through the entire process of absorption. For the pulse width of less than 429 fs the energy that might otherwise be lost to the plasma, is being absorbed and stored by the material in a superheated state at the surface. This would result in the increase of maximum surface temperature at the threshold for ablation. Hence it can be concluded that the change in trend of threshold fluence is due to complex thermodynamic processes associated with the vapor front and the bulk temperatures. Depending upon the amount of energy being absorbed in the bulk or that being extracted by the vapor front, the pulse width and the internal bulk temperature profile determines the threshold fluence. In next section, effect of pulse energy and scan speed on the thickness of deposition is discussed.

5.3 Effect of pulse energy and scan speed on width of deposition

To investigate the effect of pulse energy and scan speed on width of deposition on acceptor substrate, irradiation of gold substrate was carried out with five different scanning speeds and examined under SEM. Width of deposition increases with increase of pulse energy, as shown in Figure 5.2, while it decreases with increase of scanning speed. This is due to the fact that at high scanning speed, the laser-material interaction time is not long enough to activate the surface fully and uniformly.

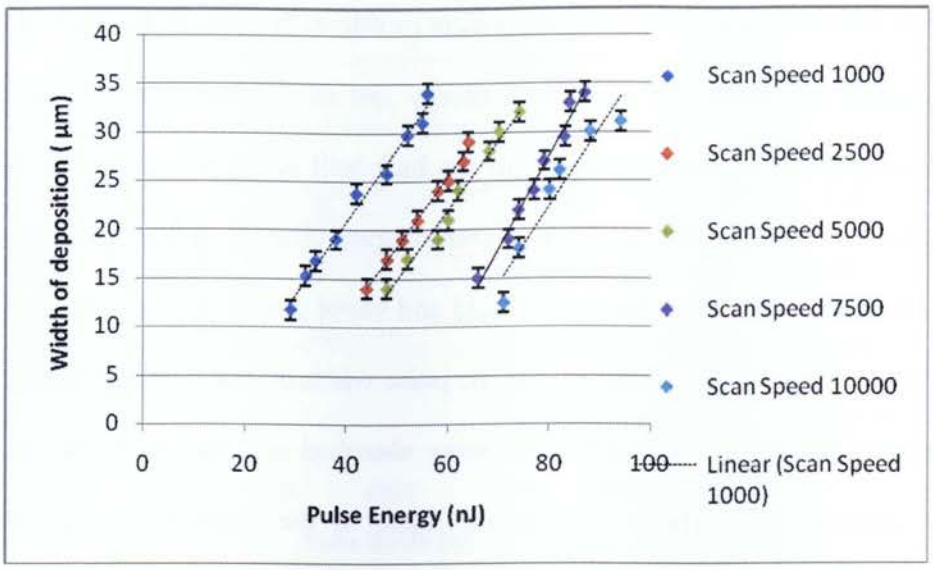

Figure5.2: Effect of pulse energy on thickness of deposition

5.4 Effect of pulse width on deposition thickness

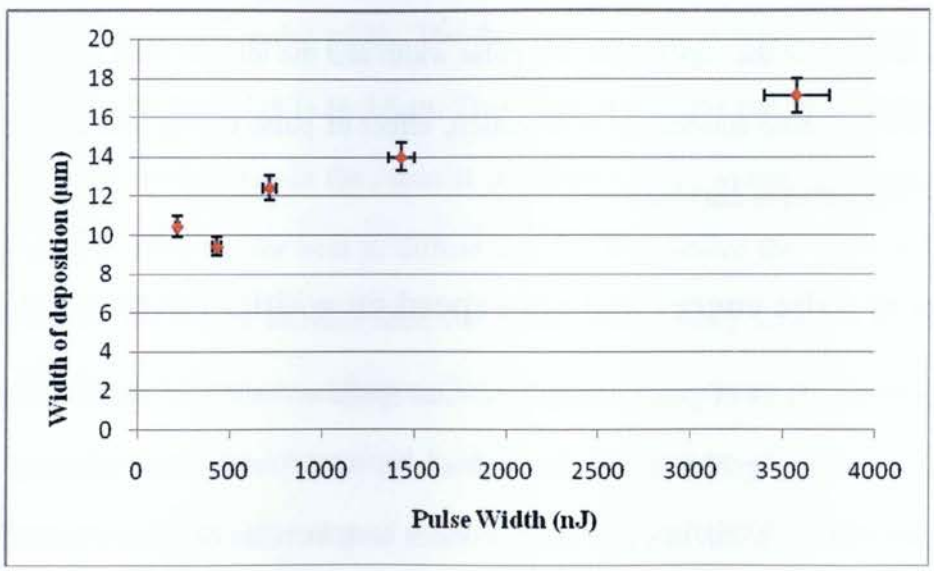

Figure5.3: Effect of pulse width on thickness of deposition

Figure 5.3 illustrates the thickness of deposition obtained at pulse widths of 214.29, 428.57, 714.29, 1428.60 and 3571.40 fs at a constant repetition rate of 26 MHz. The change in deposition thickness with pulse width can be classified regimes. In the lower regime, when the pulse width

in the range of 214.29 – 714.29 fs, the thickness increases from 10.44 μm to 12.41 μm. Further increase in pulse width from femtosecond regime to picoseconds regime, there is a little decrease in the width of deposition. Figure 5.4 shows the SEM images of deposition at a repetition rate of 26 MHz and a scan speed of 5000 μm s^{-1}. It is known that with decrease in the pulse width, peak laser intensity increases for the same pulse energy and hence a reduction in the feature size is achieved. Also, because of the small heat affected area and lower pulse energies required for femtosecond transfer [Banks et. al., 2006] than long-pulsed laser makes the transfer less violent and gentler impact on the receiver. Lower momentum impact arising from a gentler transfer can be expected to lead to less flattening and hence smaller deposited features.

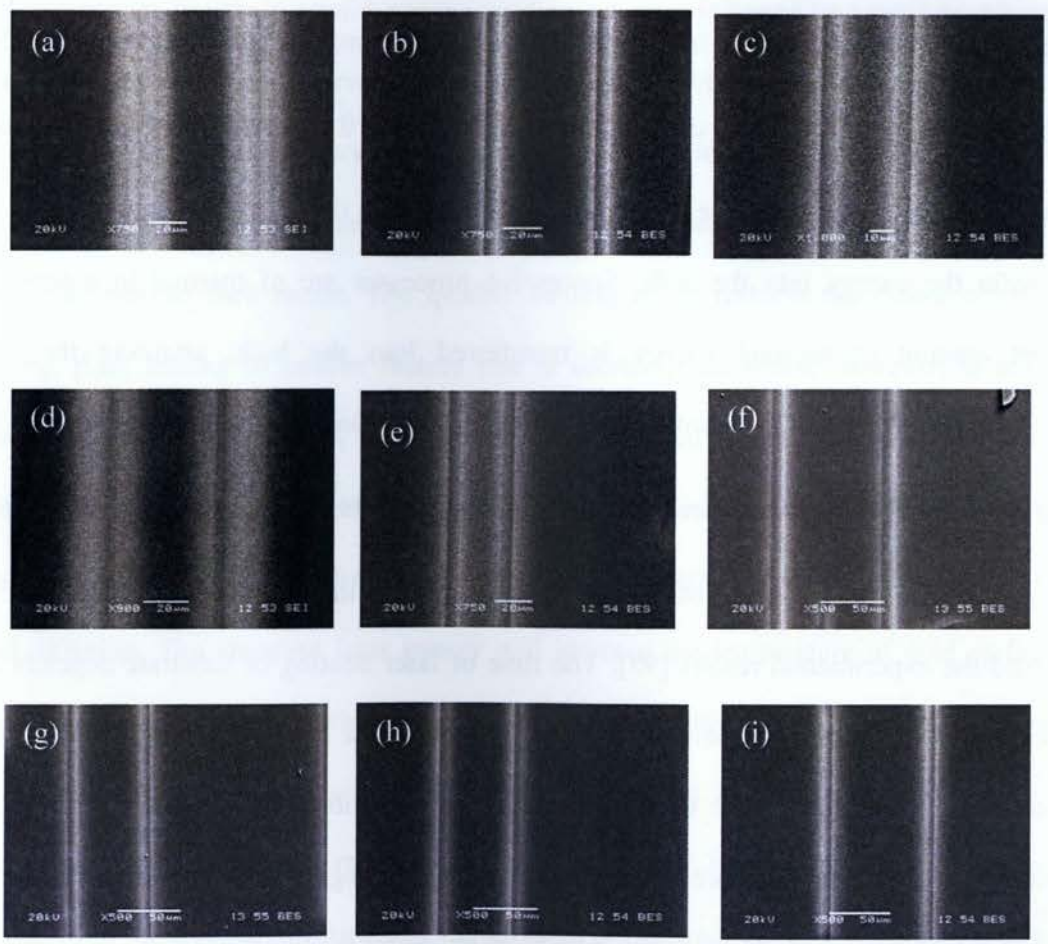

Figure 5.4: SEM pictures shows lines of transfered material in glass substrate

This phenomenon can be explained by the fact that ablation mechanism with femtosecond pulses is different from that of picosecond pulses. The difference has been extensively studied in recent years and explained qualitatively by considering the laser-solid interaction [94]. Upon impact of laser radiation on the substrate, electro-magnetic energy is converted into an electronic excitation and then into thermal energy. In other words the laser-solid interaction process is the excitation of electrons from their equilibrium states to excited states by absorption of photons. A quasi-equilibrium situation is established by electron–electron scattering on the time scale of about 10^{-13} s. At this stage, the electron temperature is much higher than the lattice temperature. Then the high temperature electrons cools off by means of emitting phonons and transferring considerable energy to the lattice on the time scale of about 10^{-12} s. After photon relaxation, the thermal diffusion from the surface to the bulk follows on the time scale of about 10^{-11} s, which can transfer the energy into the bulk. Successive processes are of thermal in nature. When sufficient amount of thermal energy is transferred into the bulk, attaining the melting temperature, transition from the solid to liquid state takes place. Therefore, the time of lattice heating by electron-phonon scattering, which is in the scale of 10^{-12} s and time of thermal diffusion, which is in the scale of 10^{-11} s in gold, are of important characteristics to better understand the experimental results [95]. The time of laser heating of substrate depends on the laser pulse duration in the laser-solid interaction. Therefore, the laser pulse duration also plays an important role in the initial laser energy deposition on the substrates surface. In Ref. [95], the time scale of energy relaxation processes with distinguished regimes of thermal and non-thermal ablation have been studied. Mechanisms leading to structural modifications using picosecond and

longer laser pulses are reported thermal in nature, which means, it takes place in timescales longer than 10^{-12} s. In contrast, femtosecond laser pulses open up non-thermal processes that take place in a timescale shorter than 10^{-12} s, i.e., before thermal processes comes into effect. In particular, with femtosecond laser pulses, ultra-fast phase transition and ablation can occur, which is different from processes with longer pulses.

In our experiments, the laser pulse duration is shorter than the silicon lattice heating time [96]. The equilibrium between electron and lattice cannot be established during laser irradiation period and even the heat diffusion is not sufficient to transfer the energy away from the surface. The deposited laser energy results directly in a solid–vapor transition, which is followed by a rapid expansion on the surface in a very short time interval. During this process, thermal diffusion into the bulk can be neglected due to the ultrashort duration. In fact, the laser ablation is a direct solid–vapor transition and the non-thermal ablation occurs. Thus accumulation of heat and vapor plume dissipates much quicker with reduced melt recast. The quicker cooling effect restricts the plume cloud to keep expanding, thus, leading to smaller feature size at shorter pulse width. However, in the case of picosecond regime (2 ps to 5 ps), the phenomenon is inversed. There is enough time to establish equilibrium between electron and lattice. And as aforementioned, thermal diffusion takes place on a time scale of 10^{-11} s and most of the deposited laser energy is transferred from surface into bulk via thermal diffusion. The absorbed laser energy will increase the temperature of gold surface. With successive pulses, gold temperature gradually reaches to the melting point. As a result the gold layer melts and a molten layer develops on the surface. Subsequent irradiation of molten layer further increases the surface temperature resulting vaporization of gold. Hence, laser ablation in this case is accompanied by the thermal diffusion and vaporization of molten layer. Therefore heat accumulation

is much faster on gold surface thus allowing the plume cloud to keep expanding. With the accompanying heat, the material in picosecond regime propagates much further than the femtosecond regime, which explains the wider deposition of gold in the picosecond regime.

5.5 Summary

The experimental analysis of the influence of change in the pulsewidth from 214 fs to 3.5 ps for high-power-high-repetition-rate femtosecond laser system was performed successfully. The ablation threshold was deduced to be a function of the pulsewidth and was found to decrease with the decrease in pulsewidth until the pulsewidth of 429 fs, after which a further decrease in pulsewidth leads to an increase in the threshold fluence. However the change is comparatively small for the range of pulsewidth selected. The deposition width did not seem to change significantly, with increase in pulsewidth. Also, the effect of pulse energy and scan speed on deposition width was performed. With the increase in pulse energy the deposition width increases and with the increase in scan speed the deposition width decreases.

CHAPTER 6 - CONCLUSIONS AND FUTURE WORK

In this chapter, the summary, conclusions and direction for future work are presented.

6.1 Summary and conclusions

To summarize, LIRT was investigated for the first time using femtosecond laser radiation for the deposition of gold structures. The experimental results presented in chapter 4 show that deposition can be obtained for fluences just above the threshold. As the pulse energy increases, a crest is formed in the deposited structure. With further increase of pulse energy, the material in the centre of the deposited structure is completely removed. Hence, the pulse energy has significant influence on material deposition. In chapter 5, the results on influence of pulsewidth, pulse energy and scan speed on thickness of deposition are presented. The width of transferred structure increases with pulse width, while it decreases with scan speed. This behaviour is explained from the energy transfer process in laser-material interaction.

In general the first time study of the laser induced reverse transfer (LIRT) technique leads to new insights of laser induced material transfer techniques. In this method, it is easy to transfer bulk materials when compared to forward transfer process where a thin film of donor substrate is essential. This technique uses less pulse energy when compared to the forward technique to ablate the donor substrate for smaller feature sizes. Further, in laser induced reverse transfer, selected areas of bulk material can be transferred and the donor substrate can be transparent or opaque. Since less laser pulse energy is required for material transfer, sensitive materials can also be transferred. This helps to vary the transferred material size by simply changing the laser processing parameters.

In the reverse transfer process, the acceptor substrate needs to be transparent for the laser to irradiate the donor substrate. But due to its simplicity, high throughput and quick processing, this technique can be used for several applications like fluidic devices, multilayer structures, transparent ohmic contacts, templates for the design of nanoporous material and masks for nonlithographic patterning. Interestingly, the transfer of gold on glass studied in the present work can be useful for fabricating chemical and biological sensors.

6.2 Future work

Since LIRT needs less laser pulse energy for material transfer, better transferred structures can be obtained using laser systems having low maximum average power by avoiding the intensity fluctuations. The experiments can be performed in various atmospheric conditions. For example, in vacuum, the material can be transferred without the influence of airborne particles during ablation hence aiding in cleaner and smooth deposition. In addition, the influence of inert gases on material transfer can also be studied. Since less energy is required for LIRT, these experiments can also be performed at lower wavelengths using third harmonics of the present laser system. The study of structural and chemical composition of deposited material using X-ray diffraction and XPS (X-ray photoelectron spectroscopy) analysis can help for efficient use of LIRT for specific applications. LIRT can be tried with protein substrates which can be useful for biomedical applications.

REFERENCES

1. R. Haight, P. Longo and A. Wagner, "Metal deposition with femtosecond light pulses at atmospheric pressure." J. Vacuum Science Technol., A Volume 21, issue 3, (2003): pp 649-652.

2. Phipps, Claude, "Laser ablation and its application." Springer series optical sciences vol. 129 (2007).

3. Bohandy, J., B.F. Kim, and F.J. Adrian, "Metal deposition from a supported metal film using an excimer laser." J. Appl. Phys. 60(4), (1986): pp. 1538-1539.

4. V. Schultze and M. Wagner, "Laser induced forward transfer of Aluminum." Applied Surface Science, 52 (1991): pp.303-309.

5. I. Zergioti, S, Mailis, N.A. Vainos, P. Papakonotantinou, C. Kalpauzos, C.P. Grigoropoulos, C. Fotakis, "Microdeposition of metal and oxide structures using ultrashort laser pulses." Applied Physics A, 66 (1998): pp. 579-582.

6. Y. Nakata, T. Okada and M. Maeda, "Transfer of laser dye by laser induced forward transfer." Jpn. J. Applied physics, 41 (2002): pp. L839-L841.

7. K. Tatah, A. Fukumoto, C.V. Thompson, "Laser ablation forward deposition of metal lines for electrical interconnect repair." (IEEE/CPMT), (1995): pp 176-178.

8. Z. Kantor, Z. Tohh, T. Szorenyi, "Deposition of micrometer-sized tungsten patterns by laser transfer technique." (1994): pp. 3506-3508.

9. S. Bae, D. Lee, H. Lee, M.Gill, B. Kim, D. Ahn (1999): pp. 159-162.

10. M. L. Levene, R.D. Scott, and B.W. Siryj, "Material Transfer Recording." Appl. Optics 9, 10, (1970): pp. 2260.

11. J. M. Karpman, M. N. Libenson, " Applications of UV lasers in Photomask-repair Technology." in Proc. of the National conf. on Application of lasers in Integrated Circuits Producing, 8, Leningrad, USSR(1973).

12. E. Fogarassy, "Basic Mechanisms and Applications of LIFT for high temperature superconducting film deposition." SPIE, 1394, 169 (1991).
13. J.A. Greer and T.E. Parker, "LIFT of metal oxides to trim the frequency of surface acoustic wafer resonator devices." SPIE 998,113 (1990).
14. J. M. Karpman, M.N. Libenson, G. P. Suslov, " Photomask Correction by UV laser Beam." Lenizdat, Leningrad, pp. 52 (1973).
15. B. Zang, Z. Guo, "Laser-induced direct deposition of thin films: Film Transfer." SPIE, 1230,406 (1990).

16. Z. Toth, Z. Kantor, P. Mogyorosi, T. Szorenvi, "Surface pattering by Pulsed laser Induced Transfer of Metals and Compounds." SPIE, 1279, 150 (1990).

17. F.J. Adrian, J. Bohandy, B.F. Kim and A. M. Jette, "A study of the Mechanism of Metal Deposition by the Laser-Induced Forward Transfer Process." J. Vac. Sci. Tech. B, 5, 5, 1490 (1987).
18. J. Bohandy, B. F. Kim, F. J. Adrian, and A. M. Jette, "Metal Deposition at 532nm Using a Laser Transfer Technique." J. Appl. Phys. 63, 4, 1158 (1988).
19. R. J. Baseman, A. Gupta, R.C. Sausa, C. Progler, "Laser and Particle-Beam Chemical Processing for Microelectronics." Mater. Res. Soc. Symp. Roc. 101, 237 (1988).
20. M. Colina, P. Serra, J.M. Fernandez-Pradas, L. Sevilla, J. L. Morenza, "DNA deposition through laser induced forward transfer." Elsevier B.V. (2004).
21. D. P. Banks, K. Kaur, R, Gazia, R. Fardel, M. Nagel, T. Lippert and R. W. Eason, "Triazene photopolymer dynamic release layer-assisted femtosecond laser-induced forward transfer with an active carrier substrate." EPL, 83 (2008) 38003.
22. C. Germain, Y. Y. Tsui, "Femtosecond Laser Induced Forward Transfer of Materials." icmens,pp.44, 2003 International Conference on MEMS, NANO and Smart Systems (ICMENS'03), (2003).

23. Yoshiki Nakata, Tatsuo Okada and Mitsuo Maeda, "Laser-induced forward transfer: the behavior of the ablated thin film in gas phase." IEEE, (1999): pp.7803,5661.
24. C. Germain, L.Charron, L. Lilge, Y. Tsui, "Electrodes for microfluidic devices produced by laser induced forward transfer." Applied Surface Science, ISSN 0169-4332, Elsevier Science, Amsterdam,(1985).
25. M. Heller, "DNA microarray technology: Devices, systems, and applications." Annu. Rev. Biomed. Eng., 4 (2002): pp. 129-153.
26. B. Tan, K. Venkatakrishnan, K. G. Tok, "Selective surface texturing using femtosecond pulsed laser induced forward transfer." Applied Surface Science, (2002).
27. Z. Kantor, Z. Toth and T. Szorenyi, "Metal pattern deposition by laser induced forward transfer." Applied Surface Science, 86 (1995): pp.196-201.
28. D. Willis, V.Grosu, "Microdroplet deposition by laser induced forward transfer." Applied Physics Letters, 86 (2005).
29. A. Pique, D. Chirsey, R. Auyeung, "A novel laser transfer process for direct writing of electronic and sensor materials." Applied Physics A, 69 (1999).
30. G. Blanchet, Y. Loo, J. Rogers and C. Fincher, "Large area, high resolution, dry printing of conducting polymers for organic electronics." Applied Physics Letters, 82 (2003): pp. 463-465.
31. W. Tolbert, I. Lee, M. Doxtader, E. Ellis and D. Dlott, "High speed color imaging by laser ablation transfer with a dynamic release layer: fundamental mechanisms." J. Imag. Sci. Tech., 37 (1993): pp. 411-421.
32. L.Yang, C. Wang, X. Ni, Z. Wang, W. Jia and L. Chai, "Microdroplet deposition of copper film by femtosecond laser-induced forward transfer." Appl. Phys. Letts, 89 (2006).
33. A. Pique D. Chrisey, B. Spargo, M. Bucaro, R. Vachet, J. Callahan, R. McGill, D. Leonhardt, and T. Mlsna, "Use of matrix assisted pulsed laser evaporation for the growth of organic thin films." (2008) pp. 421-426.

34. R. Eason, "Pulsed Laser Deposition of Thin Films." (2007) Wiley Interscience, Hoboken, New Jersey, USA.

35. A. Pique, D. Chrisey, R. Auyeng, J. Fitz-Gerald, H. Wu and M. Duignan, "A novel laser transfer process for direct writing of electronic and sensor materials." Appl. Phys. A, 69: S279-S284.

36. D. Toet, M.O. Thompson, P. M. Smith and T. W. Sigmon, "Laser-assisted silicon by explosive hydrogen release." Appl. Phys. Lett. 74, 2170 (1999).

37. Smausz, T., Hopp, B., Kecskemeti, G., and Bor, Z., (2006). "Study on metal micro-particle content of the material transferred with absorbing film assisted laser forward transfer when using silver absorbing layer." Appl. Surf. Sci. 207:365-371.

38. Blanchet, G., Loo, Y.-L , Rogers, J., Gao, F., and Fincher, C. (2003). "Large area, high-resolution, dry- printing of conducting polymers for organic electronics." Applied Physics Letters 82 (3): pp. 463-465.

39. J. Bohandy, B. Kim, F. Adrian and A. Jette, "Metal deposition at 532 nm using a laser transfer technique." J. Appl. Phys., 63(4), (1988): pp. 1158-1162.

40. Z. Toth, Z. Kantor, P. Mogyorosi, T. Szorenyi, "Surface pattering by pulsed laser induced transfer of metals and compounds." Proc. SPIEm 1279 (1990): pp. 150-157.

41. Z. Kantor, and T. Szorenyi, "Dynamics of long-pulse laser transfer of micrometer sized metal patterns as followed by time-resolved measurements of reflectivity and transmittance." J. Appl. Phys. 78(4), (1995): pp. 2775-2781.

42. H. Esrom, J. Zhang, U. Kogelschatz and A.Pedraza, "New approach of a laser-induced forward transfer for deposition of patterned thin metal films." Appl. Surf. Sci., 86 (1995): pp. 202-207.

43. S. Pimenov, G. Shafeev, A. Smolin, V. Konov and B. Vodolaga, "Laser induced forward transfer of ultra-fine diamond particles for selective deposition of diamond films." Appl. Surf. Sci., 86 (1995): pp. 208-212.

44. A. Bullock and P. Bolton, "Laser induced back ablation of aluminum thin films using picosecond laser pulses." J. Appl. Phys., 85(1), (1999): pp. 460-465.

45. L. Landstrom, J. Klimstein, G. Schrems, K. Piglmayer and D. Bauerle, "Single step patterning and the fabrication of contact masks by laser induced forward transfer." Appl. Phys. A, 78 (2004): pp. 537-548.

46. D. Willis, V. Grosu, "Microdroplet deposition by laser induced forward transfer." Appl. Phys. Lett., 86 (2005): 244103.

47. V. Grosu and D. Willis, "Evaporation and phase explosion during laser induced forward transfer of aluminum." Proc. SPIE, 5339 (2004): pp. 314-312.

48. C. Allen, J. Yarbrough, S. Bera, A. Sabbah, C. Durfee, B. Winters and J. Squier, "Optimization study of the femtosecond laser induced forward transfer process with thin aluminum films." Appl. Opt., 46(21), (2007): pp. 4650-4659.

49. R. Bahnisch, W. Gross and A. Menschig, "Single shot, high repetition rate metallic pattern transfer." Microelectron. Eng., 50 (2000): pp. 541-546.

50. L. Charron, C. Germain, L. Lilge and Y. Tsui, "Electrodes for microfluidic devices produced by laser induced forward transfer." Appl. Surf. Sci., 253 (2007), pp. 8328-8333.

51. Y. Nakata and T. Okada, "Time resolved microscopic imaging of the laser induced forward transfer process." Appl. Phys. A, 69 (1999): pp. 275-278.

52. T. Sano, H. Yamada, T. Nakayama and I. Miyamoto, "Experimental investigation of laser induced forward transfer process of metal thin films." Appl. Surf. Sci., 186 (2002): pp. 221-226.

53. A. Karaiskou, D. Papazoglou, I. Zergioti and C. Fotakis, "Shadowgraphic imaging of the sub-ps laser induced forward transfer process." Appl. Phys. Lett., 81 (2002): pp. 1594-1596.

54. A. Narazaki, T. Sato, R. Kurosaki and H. Niino, "Nano and microdot array formation by nanosecond excimer laser induced forward transfer." Appl. Phys. Exp., 1 (2008): pp. 057110.

55. G. Koundourakis, C. Rockstuhl, D. Papazoglou, A. Klini, I. Zergioti, N. Vainos and C. Fotakis, "Laser printing of active optical microstructures." Appl. Phys. Lett., 78(2001): pp. 868-870.

56. H. Yamada, T. Sano, T. Nakayama and I. Miyamoto, "Optimization of laser induced forward transfer process of metal thin films." Appl. Surf. Sci., 197-198 (2002): pp. 411-415.

57. Chichkov, B. N., et al. "Femtosecond, Picosecond and Nanosecond Laser Ablation of Solids." Applied_Physics A: Materials Science and Processing 63.2 (1997): pp. 109-115.

58. Herziger, G., E. W. Kreutz and K. Wissenbach. "Fundamentals of Laser Processing of Materials." Proceedings of SPIE - The International Society for Optical Engineering, 668, (1986): pp. 2-10.

59. Hubler, G. K., "Pulsed laser deposition." MRS Bulletin, Vol. XVII, No. 2, Feb. 92. (1992).

60. Chrisey, D.B. and Hublerm G. K., "Pulsed Laser Deposition of Thin films." eds, Wiley, New York, (1994).

61. Saegner, K. L., "Angular distribution of ablated material, Pulsed laser deposition of Thin Films." Wiley, New York, (1994): pp. 199-227.

62. Schou, J., "Laser beam-solid interactions: Fundamental aspects, in Materials Surface Processing by Directed Energy Techniques." Elsevier, (2006): pp. 33-62.

63. F. Garrelie and A. Catherinot, "Monte Carlo simulation of the laser-induced plasma-plume expansion under vacuum and with a background gas." Applied Surface Science, (2000): pp. 97-101.

64. www.ornl.gov/info/ornlreview/rev30-12.

65. Pronko, P. P., et al. "Thermophysical Effects in Laser Processing of Materials with Picosecond and Femtosecond Pulses." Journal of Applied Physics 78.10 (1995): pp. 6233-6240.

66. Chichkov, B. N., et al. "Femtosecond, Picosecond and Nanosecond Laser Ablation of Solids." Applied_Physics A: Materials Science and Processing 63.2 (1997): pp. 109-115.

67. Gamaly, E. G., A. V. Rode, and B. Luther-Davies. "Ultrafast Ablation with High-Pulse-Rate Lasers. Part I: Theoretical Considerations." Journal of Applied Physics 85.8 I (1999): pp. 4213-4221.

68. Bonse, J., et al. "Femtosecond Laser Ablation of Silicon-Modification Thresholds and Morphology." Applied Physics A: Materials Science and Processing 74.1 (2002): pp. 19-25.

69. Schäfer, C., H. M. Urbassek, and L. V. Zhigilei. "Metal Ablation by Picosecond Laser Pulses: A Hybrid Simulation." Physical Review B - Condensed Matter and Materials Physics 66.11 (2002): pp. 1154041-8.

70. Lorazo, P., L. J. Lewis, and M. Meunier. "Short-Pulse Laser Ablation of Solids: From Phase Explosion to Fragmentation." Physical Review Letters 91.22 (2003).

71. Ki Hyungson, and Jyoti Mazumder, Journal of laser applications, 17 (1999): pp. 110.

72. T.W. Trelenberg, and L.N. Dinh, Applied Surface Science, 229(2004): pp. 268.

73. Yoichi Hirayama, and Minoru Obara, Journal of Applied Physics, 97 (2005): pp. 064903.

74. L. Shah, A.Y. Arai, S.M. Eaton and P.R. Herman, "Waveguide writing in fused silica with a femtosecond fiber laser at 522 nm and 1 MHz repetition rate." Optics Express, Vol. 13, No. 6 (2005): pp. 1999-2006.

75. Physik Instrumente (PI) GmbH & Co. KG, Karlsruhe/Palmbach, Germany, (Mar. 15, 2008). http://www.physikinstrumente.com/en/products/prdetail.php?sortnr=300710

76. Special Optics, Wharton, NJ, USA, (Mar. 15, 2008).

http://www.specialoptics.com/Telecentric%20UV%20Scanning%20Lenses.html

77. Y. Dong and P. Molian, "Femtosecond pulsed laser ablation of 3C-SiC thin film on silicon." Applied Physics A: Materials Science Processing, Vol. 77, No. 6 (2003): pp. 839-846.

78. Haes A. J, W. P. Hall, L. Chang, W. L. Klein, R. P. Van Duyne, Nano Letters, 2004, (4): pp. 1029.

79. "Thin Films: Interdiffusion and Reactions." Ed. by J. M. Poate, K. Tu, and J. Meier (Wiley, New York, 1978; Mir, Moscow, 1982).

80. A. I. Stognij, N. N. Novitskii, and O. M. Stukalov, Pis'ma Zh. Tekh. Fiz.6 (2003) Tech. Phys. Lett. 43 (2003).

81. J. K. Sheu, Y. K. Su, G. C. Chi,*et al.*, Appl. Phys. Lett.74 (1999): pp. 2340.

82. Velev O. D., Tessier P. M., Lenhoff A. M. and Kaler E. W. *Nature* (1999): pp.401,548.

83. Kosiorek A, KandulskiW, Chudzinski P, Kempa K and GriersigM, *Nano Lett.*, 4 (2004): pp. 1359.

84. Jorgen Schou, Salvatore Amoruso, G. James and Lunney, "Laser Ablation and its Applications." 2006: pp. 70-74.

85. T. Hato, O. Horibe, H. Wakana, Y. Ishimaru, K. Tanabe, Physica C 426-431 (2005): pp.1489-1494.

86. Kamata, M., et al. "Materials processing by use of a Ti: Sapphire laser with automatically-adjustable pulse duration." Applied Physics A: Materials Science and Processing 79.7 (2004):pp. 1679-85.

87. Ngoi, B. K. A., et al. "Effect of energy above laser-induced damage thresholds in the micromachining by femtosecond pulse laser." Optics and Lasers in Engineering 35.6 (2001): pp. 361-9.

88. Tonshoff, H. K., et al. "Generation of periodic microstructures with femtosecond laser pulses." Second International Symposium on Laser Precision Microfabrication Singapore, (2001).

89. Le Harzic, R., et al. "Pulse duration and energy density influence on laser processing of metals with short and ultra-short pulses." Proceedings of SPIE - The International Society for Optical Engineering, 5713, (2005): pp. 115-122.

90. R. Le Harzic, D. Breitling, M. Weikert, S. Sommer, C. Fohl, S. Vallette, C. Donnet, E. Audouard and F. Dausinger, "Pulse width and energy influence on laser micromachining of metals in a range of 100 fs to 5 ps." Applied Surface Science, 2005: pp. 322-331.

91. Venkatakrishnan, K., B. Tan, and B. K. A. Ngol. "Submicron Holes in Copper Thin Film Directly Ablated using Femtosecond Pulsed Laser." Optical Engineering 40.12 (2001): pp. 2892-3.

92. Jandeleit, J., et al. "Picosecond Laser Ablation of Thin Copper Films." Applied Physics A: Materials Science and Processing 63.2 (1997): pp. 117-21.

93. Pronko, P. P., et al. "Thermophysical Effects in Laser Processing of Materials with Picosecond and Femtosecond Pulses." Journal of Applied Physics 78.10 (1995): pp. 6233-40.

94. Ngoi, B. K. A., et al. "Effect of Energy Above Laser-Induced Damage Thresholds in the Micromachining of Silicon by Femtosecond Pulse Laser." Optics and Lasers in Engineering 35.6 (2001): pp. 361-9.

95. Tonshoff, H. K., et al. "Generation of Periodic Microstructures with Femtosecond Laser Pulses." Second International Symposium on Laser Precision Microfabrication. Singapore, (2001).

96. Qiao, C. -H, et al. "Simulation Experiment of High Energy Laser Propagation in the Atmosphere." Qiangjiguang Yu Lizishu/High Power Laser and Particle Beams 20.11 (2008): pp. 1777-82.